

The background of the cover is a dynamic, abstract composition of numerous thin, glowing blue and white lines that swirl and curve across a black field, creating a sense of motion and energy. The lines vary in thickness and brightness, with some appearing as sharp, bright streaks and others as softer, more diffuse trails.

MEMBRANES AND MEMBRANE TECHNOLOGIES III

**EDITED BY
DR. JUAN MANUEL PERALTA-HERNÁNDEZ**



TRANS TECH PUBLICATIONS

Membranes and Membrane Technologies III

Edited by
Dr. Juan Manuel Peralta-Hernández

Membranes and Membrane Technologies III

Aggregated Book

Edited by

Dr. Juan Manuel Peralta-Hernández

 *Scientific.Net*

Copyright © 2024 Trans Tech Publications Ltd, Switzerland

All rights reserved. No part of the contents of this publication may be reproduced or transmitted in any form or by any means without the written permission of the publisher.

Trans Tech Publications Ltd
Seestrasse 24c
CH-8806 Baech
Switzerland
<https://www.scientific.net>

Volume 37 of
Specialized Collections
ISBN 978-3-0364-0540-7

Full text available online at <https://www.scientific.net>

Distributed worldwide by

Trans Tech Publications Ltd
Seestrasse 24c
CH-8806 Baech
Switzerland

Phone: +41 (44) 922 10 22
e-mail: sales@scientific.net

Preface

Recently, the use of membranes and related technologies has been becoming more and more popular not only in traditional fields, such as water and wastewater treatment, but also in various chemical production, including oil and gas processing, and also in modern energetic hydrogen production. It is possible without any doubt to state the fact that using membranes in processes of filtration and separation of various technological flows is a revolutionary technological trend and very promising from an economic point of view.

Let us present the next third volume of a special book series on membranes and membrane technologies, which contains articles published by Trans Tech Publications Ltd. in 2020 - 2023 years. "Membranes and Membrane Technologies III", like the previous two editions, covers a wide range of engineering solutions in the development and production of various types of membranes and their use in water and wastewater treatment, gas separation, and technological flow separation in the chemical industry.

In the preparation of this edition, a similar thematic classification by chapters was adopted as in the first two collections. This will allow the reader to quickly navigate and effectively use all editions in their professional activities.

The third special collection "Membranes and Membrane Technologies III" is presented to readers in seven chapters:

Chapter 1: Polymeric Membranes

Chapter 2: Inorganic Membranes

Chapter 3: Composite and Hybrid Membranes

Chapter 4: Technological Aspects of Membrane Water and Wastewater Treatment

Chapter 5: Complex Technologies of Water and Wastewater Treatment Using the Membrane Phase

Chapter 6: Membrane Separation in the Petrochemical and Chemical Industry

Chapter 7: Membranes and Technologies for Gas Separation

Chapter 8: Liquid Membrane Technologies

We hope that these special collections will be useful and interesting to a broad audience of researchers and engineers.

Editors:

Dr. Juan Manuel Peralta-Hernández, University of Guanajuato, Mexico

Dr. Stanislav Kolisnychenko, Trans Tech Publications Inc., Switzerland

Table of Contents

Preface

Chapter 1: Polymeric Membranes

Original Installation for Researching the Process of Forming Polysulfone Hollow Fiber Membranes T.S. Anokhina, A.Y. Raeva and I.L. Borisov	3
New Express Method of Non-Destructive Controlling of the Porous Structure of Asymmetric Membranes D.N. Matveev, I.L. Borisov and V.P. Vasilevsky	11
Facile Fabrication of Porous and Hydrophilic Polystyrene Membranes Using Recycled Waste M. Khaled, H. Noby, W.A. Aissa and A.H. El Shazly	18
Effect of Sericin Additive on Cellulose Acetate Membrane Morphology and Protein Rejection H. Waheed and A. Mukhtar	26
Analysis of the Influence of Pore-Forming Agent and Coagulation Bath on the Preparation of PES Hollow Fiber Membrane Q.Y. Jia, W.T. Sun, S.X. Liu, X. Gao, L.L. Li and C.X. Hu	32
Towards a Strategy for the Synthesis of Polymeric Ionic Liquids with a Bulk Anion in Various Reaction Media M.E. Atlaskina, A.E. Mochalova and V.M. Vorotyntsev	41
Fabrication Membrane of <i>Titanium dioxide</i> (TiO₂) Blended <i>Polyethersulfone</i> (PES) and <i>Polyvinylidene fluoride</i> (PVDF): Characterization, Mechanical Properties and Water Treatment A. Mataram, N. Anisya, N.A. Nadiyah and A. Afriansyah	48
Influence of Molecular Weight on the Morphology and Structure of Electrospun Polyvinylidene Fluoride (PVDF) A.S. Zahari, M.H. Mazwir and I.I. Misnon	55
Effect of Solvents Ratio and Polymer Concentration on Electrospun Polybenzimidazole Nanofiber Membranes Fabrication N. Nordin, I.I. Misnon, K.F. Chong, K.S. Loh and J. Rajan	61
Morphology of Micro-Porous Membrane of Waste Cigarette Butts Using Phase Inversion Method S. Setianto, L.K. Men, A. Bahtiar, B.M. Wibawa and D. Hidayat	67
Antimicrobial Assay on PVDF Nanofiber Membrane K. Kitiniyom, C. Suwanboon and N. Chanunpanich	72
Properties of Polyethersulfone Ultrafiltration Membrane by Incorporating Ionic Liquid for Humic Acid Removal A.S. Che Miur, N.F. Shoparwe, Z.A. Abdul Hamid, M.Z. Makhtar and N.I. Zainuddin	80
Properties of Polysulfone Hollow Fiber Membranes Depending on the Method of the Spinning Solution Preparing D.N. Matveev, V.P. Vasilevsky and K.A. Kutuzov	86
Preparation of Fine Porous Ultrafiltration Membranes from Polyacrylonitrile A.A. Yushkin, A.V. Balyinin, M.E. Efimov, G. Karpacheva and A.V. Volkov	92

Chapter 2: Inorganic Membranes

Vapor-Phase Axial Deposition Synthesis of SiO₂ and SiO₂-TiO₂ Sponge-Shaped Nanostructures M.C.P. Soares, E.A. Schenkel, B.F. Mendes, E. Fujiwara, M.F.M. Santos, G. Perli and C.K. Suzuki	101
--------------------------------------------------------------------------------------------------------------------------------------------------------------------------------------------------------------------------------------	-----

Processing and Characterization of UAE Clay Ceramic Membranes for Water Treatment Applications	
A.K.A. Khalil, A. Elgamouz, M.A. Atieh, A. Shanableh and T. Laoui	107
Ceramic Membrane Production from the Mixture Composition of Clay, Zeolite, Activated Carbon with Micro Particle Size	
S. Saifuddin, F. Faridah, E. Elwina and I.A. Zaz	116
The Efficiency of Pt-Doped Titania Pillared Clay Membranes for the Treatment of Real Textile Wastewater: A Case Study	
T. Choudhury	123
Microstructure and Mechanical Behavior of $\text{CaCu}_3\text{Ti}_4\text{O}_{12}$ Ceramics Hollow Fiber Prepared via Dry/Wet Spinning Method	
M. Ahmadipour, T.A. Otitoju, M. Arjmand, Z.A. Ahmad and S.Y. Pung	129
 Chapter 3: Composite and Hybrid Membranes	
Synthesis and Characterization of Electrospun Carbon Quantum Dots – Polyacrylonitrile/Polycaprolactone Composite Nanofiber Membranes for Copper (II) Adsorption	
C.M.P. Mabborang, J.N.B. Padrigo, G.M.O. Quiachon and P.A.N. de Yro	137
Kinetics and Isotherms of an Iron-Modified Montmorillonite/Polycaprolactone Composite Nanofiber Membrane for the Adsorption of Cu(II) Ions	
L.R. Somera, R. Cuazon, J.K. Cruz and L.J.L. Diaz	143
Effect of Processing Parameters on the Diameter and Morphology of Electrospun Iron-Modified Montmorillonite (Fe-MMT)/Polycaprolactone Nanofibers	
G.M.A. Tajanlangit and L.J.L. Diaz	149
Ferrite-SCNTs Composite (ZFS) Embedded Nanostructured Cellulose Acetate Membranes - A Promising Sulphate Salts Rejecting Tool. Synthesis and Characterizations	
A. Afzal, N. Iqbal and M. Rafique	158
Fabrication and Characterization of Copper-Chelated Polyethersulfone/Polydopamine Microfiltration Membrane for Antifouling Applications	
X.R.A.U. Dela Paz and R.B. Leron	174
Effect of Different Parameters on Lithium Ion Transfer through PVDF-UIO-66 Cation Selective Hybrid Membrane via Electrodialysis Technique	
A.U. Zeid, A.H. El Shazly and M.F. El Kady	179
Preparation of PVA/Chitosan/Zeolite Composite and its Antibacterial Activity for Water Treatment	
L.P. Quynh, L.N. Quang, N.K.M. Tam and L.Q. Nguyen	185
Preparation and Characterization of Polysulfone / Recam® Composite Membranes for Potable Water Production	
P. Anadão and H. Wiebeck	192
Nanozeolite-Impregnated Polysulfone/Polyethylene Glycol Nanocomposite Membrane for Ion Adsorption Application	
A.B.G. Deang, R.S.A. Alcantara, J.B. Bayot, N.K.D. Ledesma, V.L.J.L. Vasquez and J.C. Millare	197
Fabrication and Characterization of Cellulose Acetate/Organo-Montmorillonite Composite Membrane for Ion Adsorption	
S.C.J. Querijero, A.P.L. Melgar, M.C.A.M. Suba, M.M.G. Lagman, K.R. Bucud and J.C. Millare	203
Development of Carbon Nanotubes (CNTs) Membrane from Waste Plastic: Towards Waste to Wealth for Water Treatment	
L.J. Wei, T.D. Hui, A. Abd Aziz, L. Singh and N. Khodapanah	210
Effect of PVDF-Ca Ratio on Electrospun Membrane Fabrication for Water Filtration Application	
M.H. Alias, N.S. Hassin, P.P. Lau, I.I. Misnon and J. Rajan	217
Composite Membranes with a Cellulose Acetate Working Layer on a Nylon Substrate	
D.D. Fazullin	223
Studies on Antifouling Characteristic of the Magnetic Field Induced-PES-Fe_3O_4 Membrane for Water Remediation	
N.N. Tan, Q.H. Ng, E.A.R. Siti Kartini, C.W. Heah, T.L. Chew, H.P. Yong and T.W. Sigit	229

Fabrication and Characterization of Nanozeolite-Modified High Impact Polystyrene (HIPS) Membranes for Nanofiltration	
A.A. Valeros, A. Panganiban and J.C. Millare	235
Hydrophilic/Hydrophobic Property Changes on Polyacrylonitrile/Cellulose Acetate Nanofiber Membrane	
A. Kusumaatmaja, W. Nur, C. Chotimah and K. Triyana	241
Synthesis and Characterization of PVDF/Graphene Nanocomposite Membrane for Water Treatment Applications	
S. Rao, A. Lakshmikanthan, A.S. Sowmyashree, C. Hegde, A.M. Isloor and V. Malik	246
Adsorptive Removal of Multi-Metal Ions in Wastewater Using Electrospun Cellulose Acetate / Iron-Modified Nanozeolite Nanofibrous Membrane	
M.S. Tolentino, B.A. Basilia and R.R. Aquino	257
ZIF-8/Cellulose Acetate Based Mixed Matrix Membranes (MMMs) Synthesis and Characterization	
P.D. Sutrisna, C. Wijaya, C. Robby and J. Liliani	263
Chapter 4: Technological Aspects of Membrane Water and Wastewater Treatment	
Simulation Study of Reverse Osmosis Membrane for Seawater Desalination	
N.A.D. Abu Bakar, Z. Abdullah, N.H. Kasmuri, F. Subari and S.H. Hanipah	273
Developing a HEC/CMC-Reduced Graphene Oxide Hydrogel Nanocomposite for Seawater Desalination	
T. Tumolva, K.C. Madamba, I.G. Nunag and V.G. Villanueva	281
Water-Oil Separation Process Using a Porous Ceramic Membrane Module: An Investigation by CFD	
G.L.O. Neto, N.G.N. de Oliveira, F.A. Batista, G.H.d.A. Barbalho, A.M.V. da Silva, L.P.C. Nascimento, S.R.F. Neto and A.G.B. de Lima	287
Effect of Two Stages Adsorption as Pre-Treatment of Natural Organic Matter Removal in Ultrafiltration Process for Peat Water Treatment	
M. Mahmud, M. Elma, E.L.A. Rampun, A. Rahma, A.E. Pratiwi, C. Abdi and R. Rossadi	296
Study on the Effect of Applied Pressure on Iron and Manganese Rejection by Polyamide and Polypiperazine Amide Nanofiltration Membranes	
N. Kasim, E. Mahmoudi, A.W. Mohammad and S.R. Sheikh Abdullah	304
Influence of Casting Method on Pervaporational Performances of Polyheptylmethylsiloxane Membranes	
E. Grushevenko, I.A. Podtynnikov, O. Sharova, T.S. Anokhina and I.L. Borisov	312
Enhancement of Antiwetting Properties of Polystyrene Nanofibrous Membrane by Doping with Graphene Nanoplatelets	
A. Elrasheedy, M.F. El Kady, M. Bassyouni, T. Yoshitake and A.H. El Shazly	317
Investigation of Different Membrane Porosities on the Permeate Flux of Direct Contact Membrane Distillation	
A. Elrasheedy, M. Rabie, A.H. El Shazly, M. Bassyouni, A. Abdelmoneim and M.F. El Kady	323
Organosilica Multichannel Membranes Prepared by Inner Coating Method Applied for Brackish Water Desalination	
A. Aliah, M. Elma, I.F. Nata, N.A. Maulida, S.H. Fitriah, E.L.A. Rampun and A. Rahma	329
Surface Modification of PVDF Membrane Using Formic Acid for Enhance the Hydrophobicity for Desalination	
H. Agamparam and S.A. Rahman	337
Fabrication of Graphene-Modified Polyvinylidene Fluoride-co-Hexafluoropropylene Porous Polymeric Flat Sheet Membranes	
M.G. Fuko, H. Noby, A. Zkria and A.H. El Shazly	345
Performance of Mesoporous Organo Silica Membrane for Desalination	
A.E. Lestari, M. Elma, S. Rabiah, E.L.A. Rampun, A. Rahma and A.E. Pratiwi	351
Performance of Cobalt-Silica Membranes through Pervaporation Process with Different Feed Solution Concentrations	
M. Elma and G.S. Saputro	359

The Performance of Membranes Interlayer-Free Silica-Pectin Templated for Seawater Desalination via Pervaporation Operated at High Temperature of Feed Solution M. Elma, A.E. Pratiwi, A. Rahma, E.L.A. Rampun and N. Handayani	366
------------------------------------------------------------------------------------------------------------------------------------------------------------------------------------------------------------------------------------------	-----

Chapter 5: Complex Technologies of Water and Wastewater Treatment Using the Membrane Phase

Capacitive Deionization Water Desalination Technology, Process Optimization and Cost Analysis - A Review F.A. Abumadi, M. Koujan, T. Laoui, M.A. Atieh and K.A. Khalil	375
Pretreatment Process on Reverse Osmosis Brine as Electrodialysis Feed F. Taufany, R.N. Setyono, A. Wasi, I.W.R.S. Krishna, Y. Rahmawati, A. Altway, S. Susianto and S. Nurkhamidah	382
Performance Evaluation of a Novel Hydrophobic Membrane Used in a Desalination System: A Comparison between Static and Moving Configurations D. Ahmad, R. Presswell and H. Jouhara	391
Photocatalytic Degradation of Allura Red (AR) with TiO₂ Immobilized on Solution Blow Spinning (SBS) - Spun TIPP/PVP Membranes D. Dalman, K. Caquilala, K. Paquibot and N.P. Tan	397

Chapter 6: Membrane Separation in the Petrochemical and Chemical Industry

Microfiltration Performance of α-Alumina Membrane for Removal of Glycerol from Biodiesel S.P. Kusumocahyo, N.S. Maharani and S. Yusri	409
Vibratory Shear Enhanced Process Membrane Filtering Technology to Overcome the Negative Effects of Concentration Polarization A.R. Strelkov, O.V. Tsabilev and M.A. Gridneva	417
Crosslinked Sodium Alginate as a Material for Nanofiltration Protomic and Aprotomic Solvents E.S. Dmitrieva, E.E. Pankratova, T.S. Anokhina, V.V. Vinokurov and A.V. Volkov	424
Kinetics of Phase Separation Polyamic Acid (PAA) Solutions with Various Precipitants T.S. Anokhina, I.L. Borisov, A.A. Yushkin, G. Vaganov, A. Didenko and A.V. Volkov	431
Cross-Linked PIM-1 Membranes with Improved Stability to Aromatics A.A. Yushkin, A.V. Balynin, D. Bakhtin, R. Kirk, P.M. Budd and A.V. Volkov	439
Activated Natural Zeolite Membrane for Separating Dissolved Impurities in Coconut Sap H. Aripin, N. Busaeri, A.I. Gufroni and S. Sabchevski	445
Polystyrene/MWCNTs Nanofiber Membranes characterizations in Reducing Sulfur Content in Crude Oil A.H. Oleiwi, A.R. Jabur and Q.F. Alsahy	455
Self-Assembly Synthesis of ZIF-8/Polyvinylidene Fluoride(PVDF) Hybrid Membrane and its Pd (II)-Ion Extraction Behavior F. Tong, J. Gong, M.Y. Zhang, Y.J. Wang and J.L. Jiang	466
Triethylene Glycol Dehydration by Thermopervaporation G.S. Golubev, I.A. Podtynnikov, A.V. Balynin and I.L. Borisov	473
Pervaporation Separation of Toluene/TEG Mixture with PIM-1 Membrane I.A. Podtynnikov, A.V. Balynin, A.A. Yushkin, P.M. Budd, A.V. Volkov and I.L. Borisov	481

Chapter 7: Membranes and Technologies for Gas Separation

Gas Separation Membranes Based on Germanium Containing Polyalkylenesiloxane I.L. Borisov, N. Ushakov, E. Grushevenko, E. Finkel'stein and V. Volkov	489
Development of a Coating Method for Polydecylmethylsiloxane Selective Layer on Polysulfone Hollow Fiber Support I.L. Borisov, E. Grushevenko, E. Buinova and V. Volkov	495

A Review: Membrane Reactor for Hydrogen Production: Modeling and Simulation A.H. Kassi and T.A. Al-Hattab	501
Tailoring Zeolite-Composite (ZC) Impregnated Thermally Endured Nonporous Cellulose Acetate Membranes for Potential Gas Separation and Antibacterial Performances Z. Fatima, A. Afzal and S. Arshad	516
CO₂ Absorption/Desorption on Gas-Liquid Membrane Contactors Using Monoethanolamine Solvent: Comparison of Porous and Composite Hollow Fibers M.I. Kostyanaya, E.G. Novitskii and S.D. Bazhenov	532
Temperature Dependence of Hydrogen Solubility and Diffusivity in Hydrogen Permeable Membrane of Pd-Cu Alloy with B2-Type Crystal Structure H. Yukawa, S. Watanabe, A. Suzuki, Y. Matsumoto, H. Araki, M. Mizuno, K. Sugita and W. Higemoto	547
Thermal Degradation Behavior of Hydrogen Permeability of Pd-Coated V-Alloy Membrane for Hydrogen Separation and Purification H. Yukawa, T. Nambu and Y. Matsumoto	557
Thermal Decomposition Characteristics of Poly((4-Vinylbenzyl) Trimethylammonium Bis (Trifluoromethanesulfonimide)) Studied by Pyrolysis-GS / MS A.A. Atlaskin, A.A. Andronova and O.V. Kazarina	562
Oil Palm Empty Bunches Adsorber Membrane for CO₂ Reduction of Biogas TPA Gunung Kupang in South Borneo N. Hidayah, M. Elma, P.V. Darsono and I. Syaunqiah	569
The Effect of Glycerol on Alginate/Zeolite Membranes for Selectivity of CH₄/CO₂ Gas A. Suratman, R.C.M. Pratiwi, T. Suraya and E.T. Wahyuni	575
Fabrication of YSZ-Carbon Felt Composite Materials by Spark Plasma Sintering Process A. Eksatit, K. Ishii, M. Uematsu, L.H. Liu and T. Uchikoshi	583
Pebax 1657 Nanocomposite Membranes Incorporated with Nanoadsorbent Derived from Oil Palm Frond for CO₂/CH₄ Separation A.A. Ghazali, S.A. Rahman and R.A. Abu Samah	588
Introduction of Nanoscale Porous Aromatic Frameworks in PTMSP Matrix D. Bakhtin, L. Kulikov, A. Malakhov and S.D. Bazhenov	595
Synthesis and Characterization of PES/Pebax-MWCNTs Mixed Matrix Membranes for Gas Separation A.F. Yazid, H. Mukhtar and D.F. Mohshim	607
Fabrication and Characterization of PVDF/UiO-66(Zr) Mixed Matrix Membrane on Non-Woven PET Support J.R. Cementina, M.V. Torres, D.P. Bernabe, S. Lirio, M.B.M.Y. Ang and A.R. Caparanga	615
Preparation of Mixed Matrix Membranes Containing COF Materials for CO₂ Removal from Natural Gas/Review A.A. Abdulabbas, T. J. Mohammed and T.A. Al-Hattab	623
Effect of Morphology on the Permeability of CO₂ Across PSF/FCTF-1 Mixed Matrix Membranes A.A. Abdulabbas, T. J. Mohammed and T.A. Al-Hattab	635
Gas Permeation Properties of Multiwalled Carbon Nanotubes on Polyether Block Amide (Pebax-1657)/Polyethersulfone(PES) Blend Mixed Matrix Membrane for CO₂/CH₄ Separation N. Fazil, H. Mukhtar, D.F. Mohshim and R. Nasir	646

Chapter 8: Liquid Membrane Technologies

Liquid Membrane System for Extraction and Electrodeposition of Copper(II) T. Sadyrbaeva	655
Hydroxy-Functionalized PAMAM Dendrimer as a CO₂-Selective Molecular Gate for CO₂ Membrane Separation S.H. Duan, F.A. Chowdhury, T. Kai and S. Kazama	661
Design of Intelligent Network to Predicate Phenol Removal from Waste Water by Emulsion Liquid Membrane S.A.A. Akkar and S.A.M. Mohammed	668

CHAPTER 1:
Polymeric Membranes

Original Installation for Researching the Process of Forming Polysulfone Hollow Fiber Membranes

Anokhina T.S.^{a*}, Raeva A.Yu.^b, Borisov I.L.^c

Topchiev Institute of Petrochemical Synthesis, Russian Academy of Sciences,
Moscow, 119991, Russia

^atsanokhina@ips.ac.ru, ^balisa0225@mail.ru, ^cBoril@ips.ac.ru

Keywords: polymeric hollow fiber membranes, polysulfone, phase inversion, solvent, precipitant

Abstract. In this work an original installation (manipulator) has been created that allows one to obtain up to 30 samples of hollow fiber membranes in one molding cycle, while simultaneously varying the molding conditions in a wide range (polymer concentration, nature of solvent and precipitant, exposure time in air and in a precipitant environment, post-processing and washing modes samples, diameter of the carrier needle). This installation makes it possible to move to a fundamentally higher level of accumulation of experimental data on the relationship "the composition of the spinning solution - the structure of the hollow fiber membrane - the separating properties of the membrane." It will also make it possible to involve in these studies new laboratory samples of polymers whose synthesis volumes are insufficient for the existing methods of obtaining laboratory samples of hollow fiber membranes. The principle of operation of the manipulator was worked out when obtaining mini-samples of hollow fiber PSF membranes from 24 wt. % PSF solution in NMP with the addition of 19 wt. % PEG-400 blowing agent on a carrier needle with external deposition. Mini-samples were obtained for studies of morphology, mechanical, transport and separation properties in one molding cycle of the manipulator. The properties of mini-samples of hollow fiber PSF membrane were compared with the properties of a membrane made by the method of "dry-wet" molding with internal deposition from a solution of the same composition. It was found that the porous structures of the membranes differ significantly from each other. In a hollow fiber PSF membrane obtained on a manipulator, the porous structure was spongy with separate macrovoids of various shapes. However, in the membrane obtained by the "dry-wet" method, a dense selective layer was formed on the inner side of the backing layer of elongated finger-shaped pores. It is the formation of spongy pores along the entire perimeter of the fiber wall that led to a decrease in the permeability of the hollow fiber PSF membrane obtained on the manipulator. Thus, not only the composition of the solution, but also the molding method makes a significant contribution to the properties of the membrane.

Introduction

Today, an increasingly important task is the improvement of modern industrial processes in order to optimize them, reduce capital and operating costs, and negative impact on the environment. The process intensification strategy allows to solve this problem by developing new equipment, new approaches and methods that can significantly improve the flexibility of production, reduce the weight and size characteristics of the equipment, the cost of implementing the process and reduce production waste. Membrane technology is a rapidly developing area of science and technology, which is used for the separation of gases and liquids, and meets the above tasks. For the successful implementation of the separation process, membrane modules with various configurations are used: flat-frame, spiral, tubular, hollow fiber, and capillary [1]. One commonly used configuration is hollow fiber modules, into which hollow fiber membranes are bonded with epoxy resin. Hollow fiber modules are used in micro- (MF) and ultrafiltration (UF) processes in food, pharmaceutical, petrochemical industries, medicine, etc. [2] and gas separation for the production of nitrogen, oxygen, hydrogen, for removing carbon dioxide from various gas mixtures [3]. Another industrial application of MF and UF hollow fiber polymeric membranes is gas - liquid contactors for

deoxygenation of water in the semiconductor industry, ozonation of wastewater, carbonation of drinks, removal of ammonia from wastewater, etc. [4]. The main advantage of membranes in the form of hollow fibers is a higher packing density of the membrane in the module (from 3000 to 20,000 m²/m³) in comparison with flat or tubular membranes [2, 5, 6], which can significantly reduce the dimensions of the separating devices.

For the successful implementation of the membrane separation process, the membrane itself plays the main role. In general, the structure and material of the membrane must match the separation process for which the membrane was designed. Hollow fiber polymer membranes are most often obtained from natural and synthetic polymers by the solution method in the phase inversion process. [7]. Phase inversion is a phase separation process by which a polymer is transferred from a solution or melt to a solid state in a controlled manner. There are several different approaches to the implementation of the phase inversion method [6, 8], but the manufacture of hollow fiber membranes is carried out using a dry (evaporation-induced phase inversion) or wet molding method (diffusion-induced phase inversion) or their combination (dry-wet method) [9].

The initial solution, consisting of only one phase, decomposes into two: a solid polymer, which forms the matrix of the membrane, and a liquid, which forms pores in it. Due to contact with a non-solvent (precipitant), the top surface quickly precipitates, forming a dense, selective layer. This layer slows down the penetration of the nonsolvent into the polymer sublayer, which settles much more slowly and forms a more porous structure. The thermodynamic properties of the system and the kinetics of the solvent and precipitant exchange have a strong effect on the morphology of the membrane, which in turn determines its transport and separation properties. Thus, for the manufacture of hollow fiber membranes with various transport and separation properties, it is important to select a polymer, solvent, and precipitant (non-solvent) for it [8, 9]. The polymer must be soluble in the selected solvent and the solvent must be well miscible with the precipitant. Harsh non-solvents (precipitants) cause a strong supersaturation of the solution, which leads to the formation of a large number of nuclei and their rapid growth, with the formation of a fine-pore membrane [10]. The design of polymeric hollow fiber membranes depends not only on the choice of polymer, solvent and non-solvent. The deposition temperature, time to deposition and the duration of the deposition itself are all key parameters in the creation of hollow fiber membranes by the phase inversion method [11, 12].

There is a large number of scientific works on the study of the influence of the conditions of formation of hollow fibers on their membrane properties. In the review by C.Y. Fengetal 2012 collected the results of more than 160 scientific publications, including studies on 23 industrial polymers [13]. The latest review of 2019 collected studies on the influence of the nature and composition of the internal precipitant, its temperature and the contact time of the molding polymer solution with it [14].

One of the most common polymers for the manufacture of hollow fiber membranes for micro- and ultrafiltration, gas separation and membrane contactors is polysulfone (PSF) [15]. In scientific works on the formation of hollow fiber membranes from this polymer, the influence of the molecular weight and concentration of the matrix polymer, the solvent used, the type of pore-forming agent, its molecular weight and concentration, the nature and composition of the precipitant on their transport and separation properties has been studied in detail [16 - 18].

All of the above works describe the production of hollow fiber polymer membranes in laboratory dry-wet spinning machines, which is associated with obtaining a large amount of fiber, 200 m or more. The main problem is that such a large amount is not required to study the effect of molding conditions on the membrane properties of hollow fiber membranes. In addition, obtaining large volumes for research purposes entails large losses of reagents (polymer, blowing agent, solvent, and precipitant), and the time from the start of solution preparation to the formation of the membrane can take up to three days. Thus, the purpose of this work was to develop an express method for obtaining samples of hollow fiber polymer membranes using the example of small-size PSF for studying the effect of forming conditions on membrane properties.

Experimental Details

To solve this problem, in this work, an original installation (manipulator) based on a 3D printer was created, which will make it possible to obtain up to 25 mini-samples of hollow fiber membranes (Fig. 1a). The manipulator includes a block moving along the coordinates x , y , z , a carrier needle (Fig. 1b), due to the successive lowering of which mini-membrane samples will be formed into the spinning solution and precipitator, and a polymer platform with holes for containers for solutions and precipitators (Fig. 1c).

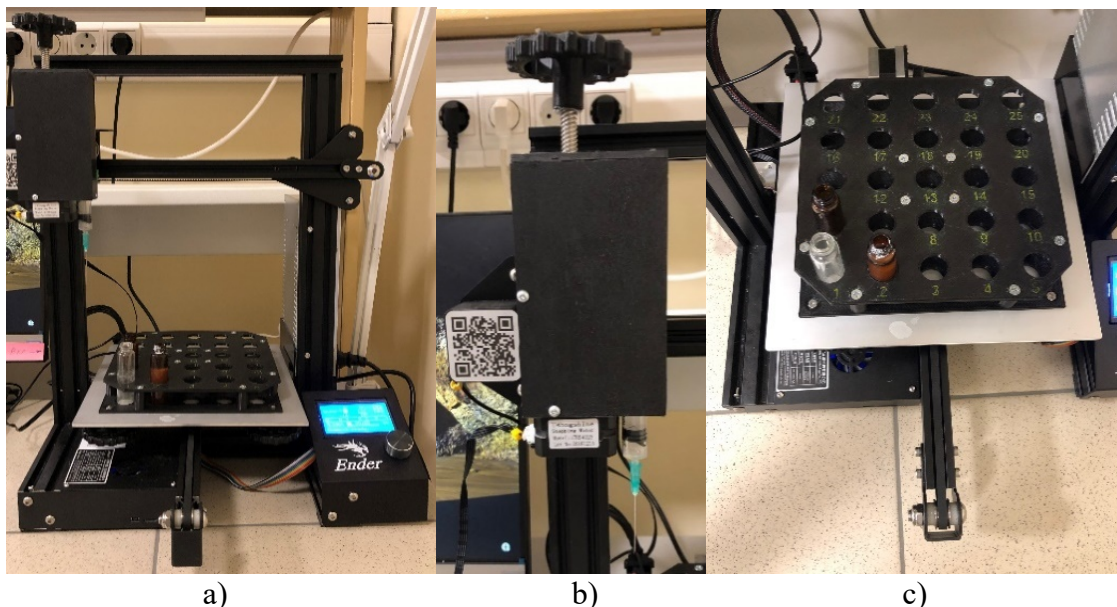


Figure 1. a) an original installation (manipulator) based on a 3D printer, which includes b) a block with a carrier needle c) a polymer platform with holes for containers for solutions and precipitants.

For the manipulator, special software has been developed that allows you to set the algorithm for the movement of the carrier needle and platform with weighing bottles for obtaining mini-samples of hollow fiber membranes. The created program allows you to set the speed of movement of the carrier needle along the coordinates x , y , z and platforms with containers for various purposes (molding solutions, precipitants, etc.), as well as the time of contact of the carrier needle with the molding solution, air and precipitant, thereby simulating modes of "wet" forming with an air gap.

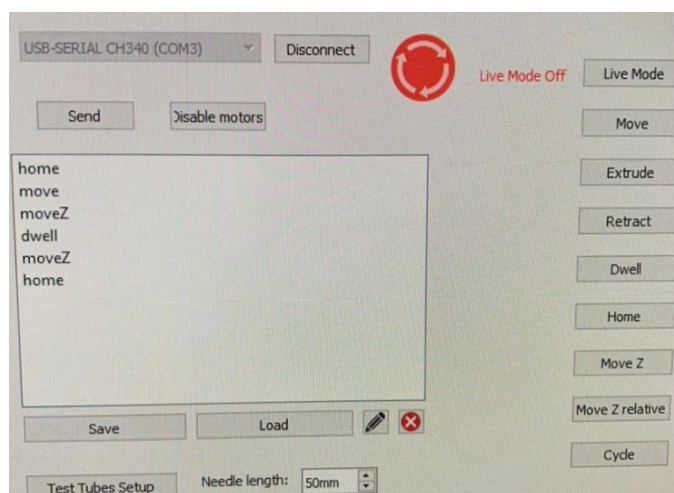


Figure 2. Software that allows you to set the algorithm for the movement of the carrier needle and platform with weighing bottles for obtaining mini-samples of hollow fiber membranes.

Were prepared 24 wt. % molding solutions PSF (BASF Ultrason® S 6010 ($M_w = 4.5\text{--}5.5 \times 10^4 \text{ g} \cdot \text{mol}^{-1}$, BASF, Germany) in N-methylpyrrolidone (NMP) with a polyethylene glycol (PEG) content ($MW = 400 \text{ g} / \text{mol}$) from 19 wt%. The viscosity of the solution was investigated using a Brookfield DV III-Ultra rotary viscometer at a temperature of 25°C . The kinetics of solution deposition was measured using the “limited” layer method, which is described in detail in [19].

Using the created manipulator, from the molding solution, mini-samples of hollow fiber PSF membranes with external deposition were made to study the morphology, mechanical and transport properties.

Scanning electron microscopy (SEM) was used to characterize the structure and morphology of the membranes. SEM was carried out on a Thermo Fisher Phenom XL G2 Desktop SEM (USA). Cross-sections of the membranes were obtained in liquid nitrogen after preliminary impregnation of the specimens in isopropanol. A thin (5-10 nm) gold layer was deposited on the prepared samples in a vacuum chamber ($\sim 0.01 \text{ mbar}$) using a desktop magnetron sputter "Cressington 108 auto Sputter Coater" (UK). The accelerating voltage during images acquisition was 15 keV. Further images analysis and determination of the selective layer thickness was carried out using the Gwyddion software (ver. 2.53).

The morphology of hollow fiber PSF membranes was investigated by the dry-wet spinning method as follows. The structure and morphology of PAA membranes were studied on a Tabletop TM 3030 Plus electron microscope (Hitachi, Krefeld, Germany). The samples were transversely cleaved in liquid nitrogen to analyze the structure of the membrane. A thin conductive gold layer was deposited on the surface before placing the samples inside the microscope chamber. The accelerating voltage was 3–5 kV

Investigations of mechanical characteristics were carried out using a TT-1100 tensile testing machine (Cheminstruments, USA) at room temperature ($22 - 24^\circ \text{C}$). The traverse speed was $3.8 \text{ cm} / \text{min}$. The samples were pieces of rectangular films with a length of about 70 mm and a width of about 10 mm. The initial distance between the clamps was 50..60 mm. The modulus was determined from the slope of the initial, close to straight-line section of the stress-strain dependence at strain values not exceeding 5%. The calculation of stresses was carried out on the initial section of the sample.

The study of the permeability of the obtained mini-sample of PSF hollow fiber membrane was carried out on a setup (Fig. 3), which includes a pump, a hose system, flowmeters and pressure sensors. The mini-sample was sealed into the module and, in a flow-through mode under pressure, the permeate was collected into weighing cups, which were then weighed, and the collection time was recorded.



Figure 3. Installation for measuring water permeability and retention capacity.

Calculations of permeability and the rejection were calculated in the same way as described in [20]. To measure the retention coefficient, an aqueous solution of Blue Dextran MM (Sigma Aldrich) = 70,000 g/mol with a concentration of 100 mg / kg was prepared and used.

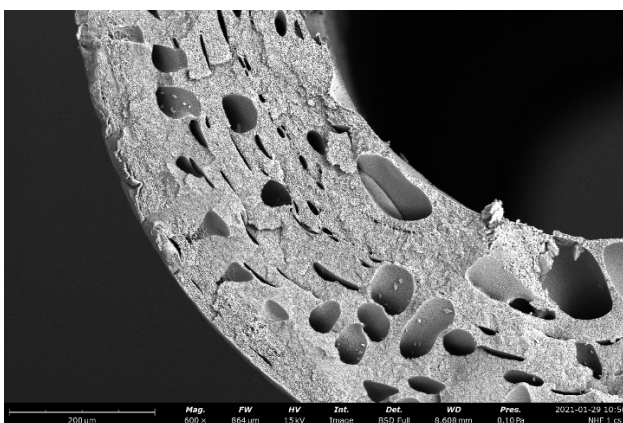
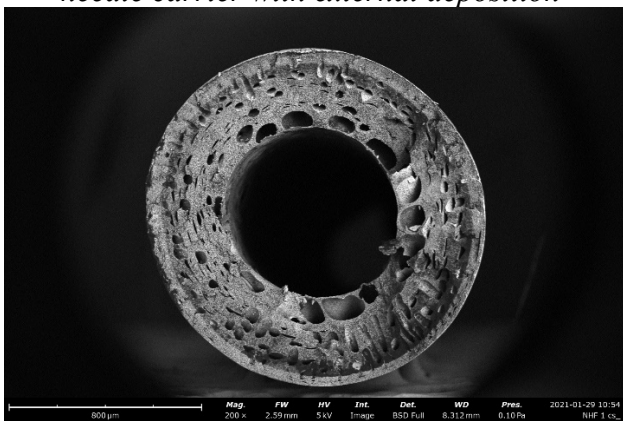
The results obtained were compared with a sample of a PSF hollow fiber membrane obtained from the same solution using the method of “dry-wet” formation of membranes made on a laboratory setup [20].

Results and Discussion

For the prepared solution, the viscosity, rate and settling time were investigated. The viscosity of the solution was 34500 mPa·s, while the deposition rate was 24/19 wt. % PSF / PEG solution in NMP in a “limited” layer with a thickness of 350 μm was 14 μm / s, the settling time of the solution corresponded to 24 s. The settling time of a polymer solution with a certain thickness is an important value in the formation of a hollow fiber membrane, since it allows us to understand how much of a carrier needle should be at least in a bottle with a polymer solution.

After determining the properties of the spinning solution, mini-samples of hollow fiber membranes were made from it. SEM photographs of the resulting membrane are shown on the left in Figure 4.

Hollow fiber PSF membrane obtained on a needle carrier with external deposition



Hollow fiber PSF membrane obtained by "dry-wet" forming with internal deposition

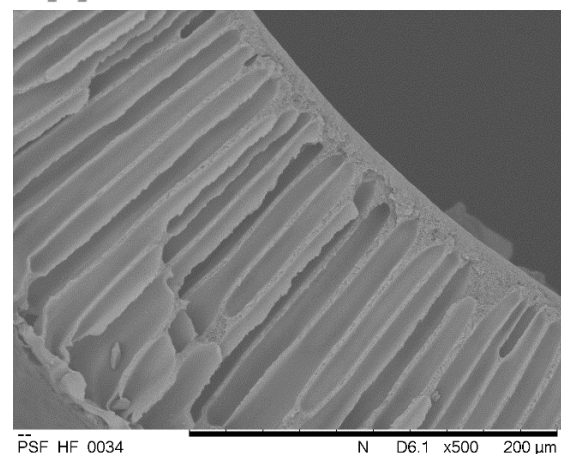
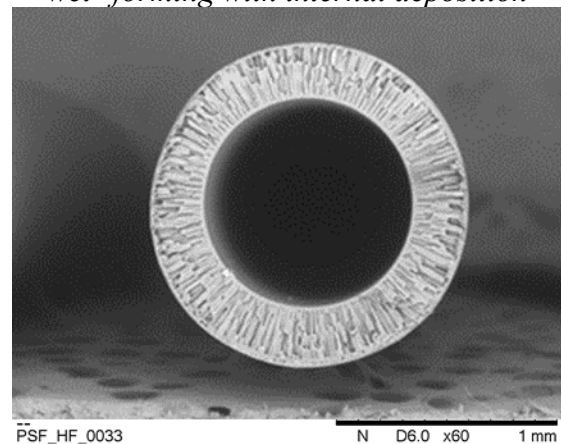


Figure 4. SEM photographs of hollow fiber PSF membranes made on a carrier needle with external deposition (left) and by “dry-wet” forming with internal deposition (right).

SEM photographs show that the porous structure of hollow fiber PSF membranes obtained from the same molding solutions differs significantly from each other. In a hollow fiber PSF membrane, when manufactured by the method of “dry-wet” molding with internal deposition, a selective layer and a layer with long finger-like pores with a diameter of about 15 μm are formed on the inside. At the same time, a spongy structure with separate microvoids of various shapes

(rounded, vertically and horizontally elongated) with a diameter of 30 μm prevails in the hollow fiber PSF membrane obtained using a new manipulator on a carrier needle with external deposition. Such a difference in the porous structure can be associated with the presence of a carrier needle in the case of obtaining hollow fiber PSF membranes using a manipulator. Then, as in the case of a membrane made by the method of “dry - wet” forming with deposition from the inside, the precipitant, passing through the polymer layer, encounters air, the resistance of which is negligible compared to the resistance of stainless steel of the carrier needle.

A mini-sample of the hollow fiber PSF membrane obtained on the manipulator was characterized in terms of mechanical properties, water permeability (Fig. 5) and retention of the Blue Dextran model dye ($\text{MM} = 70 \text{ kg / mol}$). The strength of the hollow fiber PSF membranes obtained on the manipulator was 15 MPa.

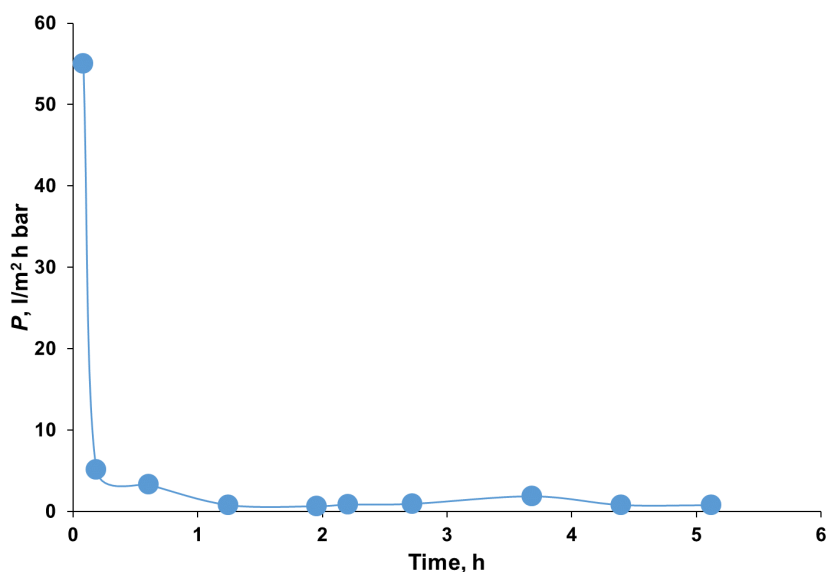


Figure 5. Time dependence of permeability of a mini-sample of a hollow fiber PSF membrane obtained on a manipulator.

Permeability of a hollow fiber PSF membrane obtained from 24/19 wt. % PSF / PEG solution in NMP on a new manipulator using a carrier needle, corresponded to approximately 1 $\text{l/m}^2 \text{ h atm}$. For a membrane obtained from the same solution, but using the “dry-wet” molding method, the membrane permeability was 82 $\text{l/m}^2 \text{ h atm}$ [20]. This difference in the permeabilities of hollow fiber PSF membranes can be explained in terms of the emerging porous structure. As mentioned above, in an internally deposited membrane, a thin selective layer is formed on a support layer of long finger-shaped pores. It is the thickness of the selective layer that is responsible for the value of the membrane permeability. The thinner the layer, the higher the permeability and vice versa. In this case, the backing layer does not introduce resistance to the water flow through the membrane, since the finger-like pores have a straight elongated shape.

In the case of a hollow fiber PSF membrane obtained with external deposition on a carrier needle, a spongy structure prevails over the entire thickness. That is, despite the fact that in such a membrane the porosity can be much higher, the entire wall thickness of the hollow fiber contributes to the permeability due to the large tortuosity of the pores, and accordingly the resistance arising from this tortuosity.

Thus, it can be concluded that not only the composition of the molding solution, but also the molding method play an important role both in the porous structure of the final membrane and in their permeability.

The study of the release properties showed that the mini-sample of the hollow fiber PSF membrane obtained on the manipulator has a high rejection of the Blue Dextran model dye ($\text{MM} = 70,000 \text{ g / mol}$) 99.9%.

Conclusion

In this work an original installation (manipulator) has been created that allows one to obtain up to 30 samples of hollow fiber membranes in one molding cycle, while simultaneously varying the molding conditions in a wide range (polymer concentration, nature of solvent and precipitant, exposure time in air and in a precipitant environment, post-processing and washing modes samples, diameter of the carrier needle). This installation makes it possible to move to a fundamentally higher level of accumulation of experimental data on the relationship "the composition of the spinning solution - the structure of the hollow fiber membrane - the separating properties of the membrane." It will also make it possible to involve in these studies new laboratory samples of polymers whose synthesis volumes are insufficient for the existing methods of obtaining laboratory samples of hollow fiber membranes. The principle of operation of the manipulator was worked out when obtaining mini-samples of hollow fiber PSF membranes from 24 wt. % PSF solution in NMP with the addition of 19 wt. % PEG-400 blowing agent on a carrier needle with external deposition. Mini-samples were obtained for studies of morphology, mechanical, transport and separation properties in one molding cycle of the manipulator. The properties of mini-samples of hollow fiber PSF membrane were compared with the properties of a membrane made by the method of "dry-wet" molding with internal deposition from a solution of the same composition. It was found that the porous structures of the membranes differ significantly from each other. In a hollow fiber PSF membrane obtained on a manipulator, the porous structure was spongy with separate macrovoids of various shapes. However, in the membrane obtained by the "dry-wet" method, a dense selective layer was formed on the inner side of the backing layer of elongated finger-shaped pores. It is the formation of spongy pores along the entire perimeter of the fiber wall that led to a decrease in the permeability of the hollow fiber PSF membrane obtained on the manipulator. Thus, not only the composition of the solution, but also the molding method makes a significant contribution to the properties of the membrane.

Acknowledgements

This work was funded by the Russian Science Foundation, Russia (Project no. 20-79-00343).

References

- [1] Dr. Suzana Pereira Nunes Dr. Klaus-Viktor Peinemann, Membrane Technology: in the Chemical Industry, Second, Revised and Extended Edition. Wiley-VCH Verlag GmbH & Co. KGaA, (2006) 340.
- [2] A. Cassano, A. Basile. Membranes for industrial microfiltration and ultrafiltration. Woodhead Publishing Limited, (2011) 647 – 679.
- [3] P. Bernardo, E. Drioli, G. Golemme. Membrane Gas Separation: A Review/State of the Art. Ind. Eng. Chem. Res, 48 (2009) 4638–4663.
- [4] A.K. Pabby, A.M. Sastre. State-of-the-art review on hollow fibre contactor technology and membrane-based extraction processes. J. Mem. Sci., 430 (2013) 263-303.
- [5] D. de Montigny, P. Tontiwachwuthikul, A. Chakma, Using polypropylene and polytetrafluoroethylene membranes in a membrane contactor for CO₂ absorption. J. Mem. Sci., 277 (2006) 99-107.
- [6] A.V. Bilydukevich, T.V. Plisko, V.V. Usosky. The formation of polysulfone hollow fiber membranes by the free fall spinning method. Petroleum Chemistry, 56 № 5 (2016) 379-400.
- [7] R.W. Baker. Overview of membrane science and technology. Membrane technology and application, (2004) 535.

-
- [8] B.S. Lalia, V. Kochkodan, R.Hashaikeh, N. Hilal. A review on membrane fabrication: Structure, properties and performance relationship. *Desalination*, 326 (2013) 77–95.
- [9] M. Cheryan, P.A. Lancaster, M. Cheryan, *Ultrafiltration and Microfiltration Handbook*. USA: Technomic Publishing Company, (1998) 552.
- [10] L. P. Perepechkin. Methods for Obtaining Polymeric Membranes. *Russian Chem. Rev.*, 57 № 6 (1988) 539–548.
- [11] G.R. Guillen, G.Z. Ramon, H.P. Kavehpouretal. Direct microscopic observation of membrane formation by nonsolvent induced phase separation. *J. Mem. Sci.*, 431 (2013) 212-220.
- [12] M. Sadrzadeh, S. Bhattacharjee. Rational design of phase inversion membranes by tailoring thermodynamics and kinetics of casting solution using polymer additives. *J. Mem. Sci.*, 441 (2013) 31-44.
- [13] C.Y. Feng, K.C.Khulbe, T.Matsuura, A.F.Ismail, Recent progresses in polymeric hollow fiber membrane preparation, characterization and applications. *Sep. Pur. Tech.*, 111 (2013) 43–71.
- [14] A.L. Ahmad, A. O. Tunmise, S.O. Boon. Hollow fiber (HF) membrane fabrication: A review on the effects of solution spinning conditions on morphology and performance. *J. Ind. Eng. Chem.*, 70 (2019) 35–50.
- [15] S. Kheirieh, M. Asghari, M. Afsari. Application and modification of polysulfone membranes. *Rev. Chem. Eng.*, 34 № 5 (2018) 657–693.
- [16] T. V. Plisko, A. V. Bilyukevich, V. V. Usosky, V. V. Volkov. Influence of the Concentration and Molecular Weight of Polyethylene Glycol on the Structure and Permeability of Polysulfone Hollow Fiber Membranes. *Petr. Chem.*, 56 № 4 (2016) 321–329.
- [17] A.V. Bilyukevich, T.V. Plisko, G.A. Branitskii, N.G. Semenkevich, I.L. Zharkevich. Investigation of the Morphology of Polymer–Inorganic Capillary Membranes Based on Polysulfone. *Petr. Chem.*, 53 № 7 (2013) 521–528.
- [18] P.S.T. Machado, A.C. Habert, C.P. Borges. Membrane formation mechanism based on precipitation kinetics and membrane morphology: flat and hollow fiber polysulfone membranes. *J. Mem. Sci.*, 155 (1999) 171-183.
- [19] T. Anokhina, I. Borisov, A. Yushkin, G. Vaganov, A. Didenko, A. Volkov. Phase Separation within a Thin Layer of Polymer Solution as Prompt Technique to Predict Membrane Morphology and Transport Properties. *Polymers*, 12 №12 (2020) 2785.
- [20] T.S.Anokhina, S.D.Bazhenov, I.L.Borisov, V.P.Vasilevsky, V.A.Vinokurov, A.V.Volkov. Nanocellulose as Modifier for Hollow Fiber Ultrafiltration PSF Membranes. *Key Engineering Materials*, 816 (2019) 238-243.

New Express Method of Non-Destructive Controlling of the Porous Structure of Asymmetric Membranes

MATVEEV Dmitry^{a*}, BORISOV Ilya^b, VASILEVSKY Vladimir^c

A.V. Topchiev Institute of petrochemical synthesis RAS, Moscow, Russia

^admatveev@ips.ac.ru, ^bBoril@ips.ac.ru, ^cvasilevskii@ips.ac.ru

Keywords: Express method, porous structure, high-intensity electric fields, polymer membranes, pore size distribution.

Abstract. An important practical and fundamental problem in the production of porous polymer membranes is the study of the porous structure and the detection of "defects" or large pores in the area of the membrane. Known porosimetry methods cannot solve this problem. This work proposes a new non-destructive express method for studying the porous structure of asymmetric polymer membranes in high-intensity electric fields. This method can be successfully implemented on both flat sheet and hollow fiber membranes with a known porous structure. On the example of hollow fiber membranes made of polyacrylonitrile and polysulfone an assessment of the chemical structure effect of the membrane material on the high-voltage discharge currents in a highly inhomogeneous electric field through hollow fiber membranes with a given pore size was made. Under normal conditions and an average intensity of an inhomogeneous electric field $E = 5$ kV/cm, the results obtained allow us to conclude about a certain practical potential of the developed express method.

Introduction

Porous membranes are widely used in micro, ultra and nanofiltration, gas-liquid contactors, etc. [1-5], and as support for forming composite membranes with a thin separating layer [6-7]. Structural and transport characteristics (permeability and selectivity) are most important for membrane selection as they provide information on how the membrane will perform in the intended separation process. When choosing a membrane for a particular technological application and especially to determine the optimal modes of membrane formation at the stage of its development and production, it is important to analyze both the pore size of the membrane [8] and the homogeneity of its porous structure in extended areas with geometric localization of possible defects.

Modern membrane gas separation is based on polymeric hollow fiber membranes with an outer diameter of 400-500 microns. Polymer hollow fiber membranes have several advantages over flat membranes, such as a high surface area to volume ratio, ease of manufacturing a membrane module, high packing density per unit volume in a membrane module, and a small area of membrane equipment [9-11]. To obtain composite hollow fiber membranes with a thin separation layer, highly permeable support with a controlled porous structure are required. Optimization of such a porous structure is impossible without a fast and reliable method for characterizing the size of membrane transport pores.

Among the traditional methods of membrane characterization, electron microscopy, physical methods for determining the membrane pore size and pore size distribution, and methods based on the analysis of the values of permeability and retention of solutions of reference molecules or particles can be distinguished [12]. Electron microscopy methods are represented by scanning electron microscopy SEM, transmission electron microscopy TEM, atomic force microscopy AFM, etc. Physical methods for determining pore size and pore size distribution are well known: bubble point and flow porosimetry, porosimetry based on the principle of mutual displacement of liquids, mercury porosimetry, equilibrium vapor sorption, displacement of liquid by gas (permporosimetry), analysis of liquid-solid thermograms during phase transition of liquid in membrane pores (thermporosimetry) [13-17]. Methods that measure the rejection of model molecules by the

membrane provide information on the structural properties of the membrane based on models based on the concept of the pore shape and regularities of mass transfer through a porous medium [9, 18-19].

When using these methods, researchers, as a rule, attribute the obtained data to the entire characterized membrane, which, in the absence of information about the homogeneity of the porous structure over the area or length of the characterized sample, often leads to obvious errors.

In connection with the above, an urgent task of membrane science and technology is the creation of a new express method of non-destructive testing of both the regular porous structure of the membrane and local defects of the membrane. In this work, we propose such a method, the essence of which is that a weak electric discharge is excited in the pore space of the membrane with the help of a system of electrodes. The generated flow of charged particles (for example, electrons) moves through the pore space of the membrane under the action of the electric field forces and is recorded as a current in the electrode circuit. This express method allows to check both the regularity of the porous structure of the membrane as a whole, and to identify its characteristic areas for the subsequent targeted preparation of samples for their study by the above "destructive" research methods.

Experimental Details

The proposed method for studying the porous structure is suitable for both flat sheet membranes (Fig. 1a) and hollow fibers (Fig. 1b).

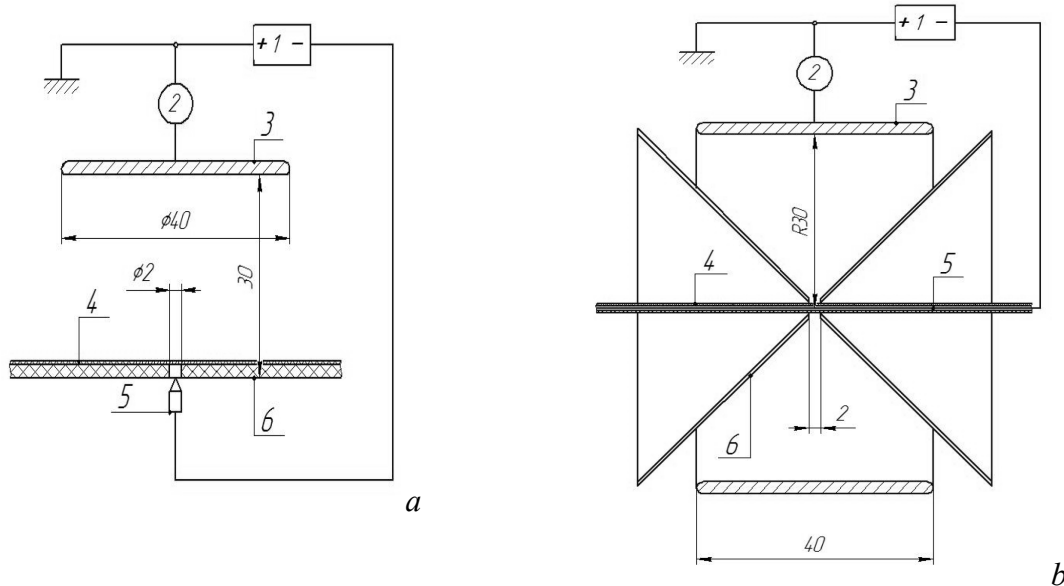


Fig. 1. Laboratory setup for studying the homogeneity of the porous structure of flat sheet (a) (hollow fiber (b)) membranes. 1- high voltage source; 2 - microammeter; 3 - disk (ring) anode; 4 - investigated flat sheet (hollow fiber) membrane; 5 - corona cathode (string); 6 - subject table (lens hood).

Fig. 1a schematically shows a built laboratory setup for studying the homogeneity of the porous structure of flat sheet membranes. This variant uses an inhomogeneous electric field in the "needle - plane" electrode system. The corona discharge current under normal conditions depends on the pore size and porosity in the elementary section of the membrane under study, limited by a diaphragm hole of $\text{Ø} 2$ mm. When the membrane moves in the plane of the figure from left to right with a discrete step of 2 mm, the "line" dependence of the discharge current on the discrete number of the element of the "line" under study is removed. The procedure is repeated with subsequent displacements of the membrane perpendicular to the plane of the drawing by 2 mm. Thus, a "line-by-line" scan of the investigated section of the membrane is obtained with data on the corona discharge current for each scan element with a resolution of 2 mm over the membrane surface. The

object of the study was a microfiltration hydrophobic flat sheet membrane MFFK-5 (ZAO STC Vladipor, Russia) with an average pore size of 0.8-1.2 μm .

In Fig. 1b schematically shows a variant of a laboratory setup for the homogeneity studying of the porous structure of hollow fiber membranes. In this case, an inhomogeneous electric field is used in the "string - coaxial cylinder" electrode system. Here, the corona discharge current under normal conditions depends on the pore size and porosity in an elementary annular section of the membrane under study, bounded by a 2 mm wide slit of a pair blend. When the membrane with the corona wire moves in the plane of the figure from left to right with a discrete step of 2 mm, the dependence of the discharge current on the discrete element number of the length of the membrane under study is removed. As an object of research, we used hollow fiber membranes made of polyacrylonitrile (PAN) and polysulfone (PSF).

Hollow fiber membranes made of PAN and PSF were obtained by the method of dry-wet phase inversion in the variant of "free spinning" of a hollow fiber in air with the supply of an coagulant (water) inside the liquid capillary of a polymer solution, in which the formed hollow fiber under its own weight enters the receiving tank, where spontaneously reels into the bay. Before the process of forming the hollow fiber membranes, the casting solution was subjected to a filtration procedure. For this, the solution was heated to 40 $^{\circ}\text{C}$ in order to reduce its viscosity in order to shorten the filtration time, after which the spinning solution was filtered under a nitrogen pressure of 1.8-2.0 bar through a stainless steel mesh with a mesh of 4-5 μm . After the filtration procedure, the casting solution was cooled to room temperature and subjected to a vacuum degassing process. The obtained samples of hollow fiber membranes were washed sequentially with tap water, then with ethanol for 2 h, then with n-hexane for 2 h, and then dried in air. The membrane post-treatment procedure was used to prevent capillary pore contraction [20].

The pore size distribution in the membranes was determined on POROLIQ 1000 ML equipment. The principle of operation of the device is based on the displacement of a non-wetting liquid. Wetting and non-wetting liquids were saturated solutions of water in isobutanol and isobutanol in water, respectively.

Geometric parameters and morphology of the structure of the hollow fiber membranes were examined by scanning electron microscopy (SEM) using a microscope Hitachi Tabletop TM 3030 Plus with a highly sensitive detector of low vacuum of the secondary electrons (Hitachi High Technologies Corporation, Japan). Chipped samples were obtained in liquid nitrogen, and then coated with a layer of gold using DSR -1 (NSC, Iran). The thickness of the gold film layer varied from 50 to 100 angstroms.

Results and Discussion

The main idea of the laboratory setup is to use the properties of a corona discharge arising in a sharply inhomogeneous electric field near an electrode with a large curvature of the surface (points, thin wires). The area near such an electrode is characterized by significantly higher field strengths compared to the average values for the entire interelectrode gap. When the near-electrode field strength of about 30 kV/cm (for air) is reached, an ionization glow in the form of a "corona" appears around the electrode, shifted to the ultraviolet region of the spectrum. The mechanism of air ionization with different polarity of the corona electrode is also different. A corona cathode was used in this work. In this case, the carriers of current in the outer region of the discharge are negative ions and the occurrence of unwanted streamers and spark discharges is excluded.

A microfiltration hydrophobic flat sheet membrane MFFK-5 with an average pore size of 0.8-1.2 μm was investigated in the mode in accordance with Fig. 1a at a high voltage of 15 kV and normal conditions. Fig. 2 shows the results of a one-line measurement of the corona discharge current depending on the measurement coordinate. At the coordinate of 20 mm, a model defect in the form of a puncture with a needle with an outer diameter of 0.2 mm was applied to the membrane.

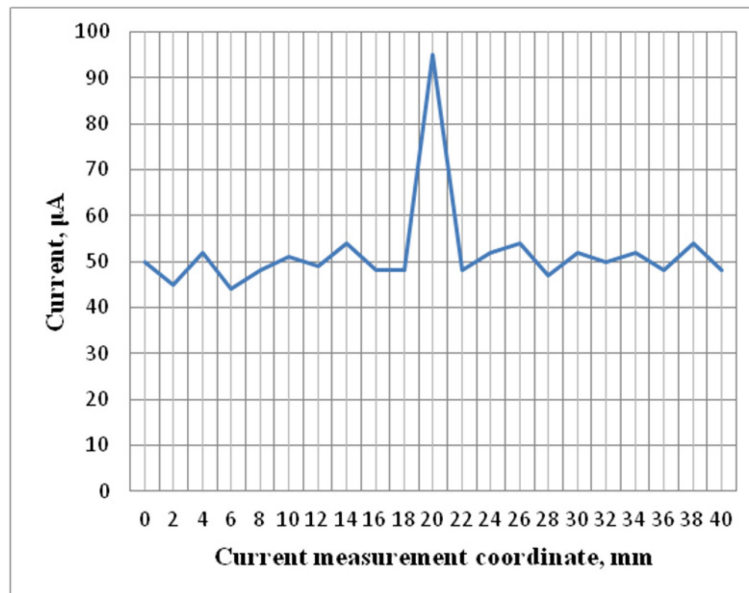


Fig. 2. Dependence of the corona discharge current on the measurement coordinate in the case of a MFFK-5 flat sheet membrane.

The data presented in Fig. 2 demonstrate the practical possibility of using the new method for monitoring the homogeneity of the porous structure of flat sheet membranes with the detection and geometrical localization of defects.

A hollow fiber PSF membrane obtained with an elongation ratio of 1.2 [21], with an average pore size of 19 nm was investigated in the mode in accordance with Fig. 1b at 15 kV high voltage and normal conditions. Fig. 3 shows the results of measuring the corona discharge current depending on the measurement coordinate along the fiber length. At the coordinate of 20 mm, a model defect in the form of a puncture of the fiber wall with a needle with an outer diameter of 0.2 mm was applied to the hollow fiber membrane. From Fig. 3 it is seen that, as in the case of the flat sheet membrane, the new method makes it possible to control the homogeneity of the porous structure of the hollow fiber membrane with the localization of detected defects.

An assessment of the effect of the chemical structure of the material on high-voltage discharge currents in a highly inhomogeneous electric field through membranes with a given pore size was made. The evaluation was carried out using two types of hollow fiber membranes: PAN and PSF. Fig. 4 shows cross-sectional SEM images of the respective hollow fiber membranes. It can be seen that the membranes have an asymmetrical structure with two thin selective layers (inner and outer sides of the hollow fiber) and the intermediate porous layer permeated finger-type macrovoids in case of PSF membranes and large vacuoles in the case of hollow fiber from PAN. From the SEM images (Fig. 4) were estimated mean values of geometrical parameters of the fibers, such as external and internal diameter (D_{out} and D_{int}), fiber wall thickness d (Table 1). Evaluation of these parameters of hollow fiber membranes makes it possible to judge the dimensional admissibility of the investigated hollow fiber membranes in relation to the proposed method for studying the porous structure in high-intensity electric fields.

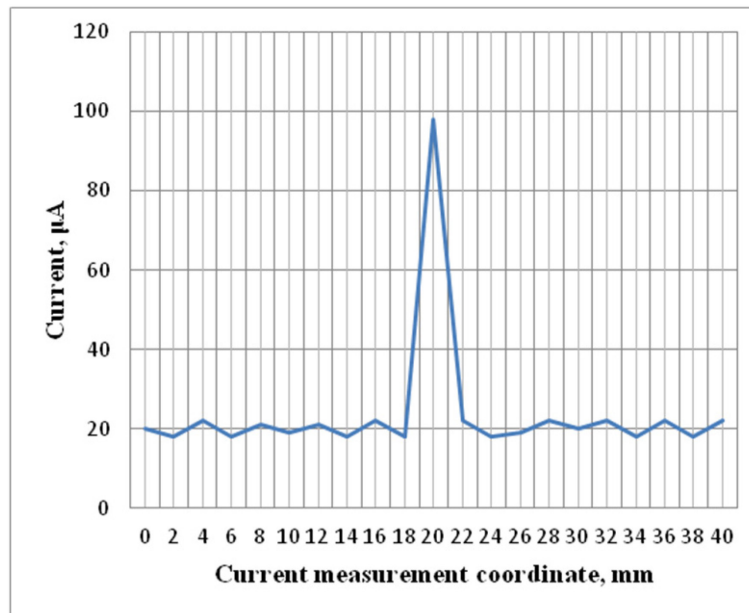


Fig. 3. Dependence of the corona discharge current on the measurement coordinate in the case of a PSF hollow fiber membrane.

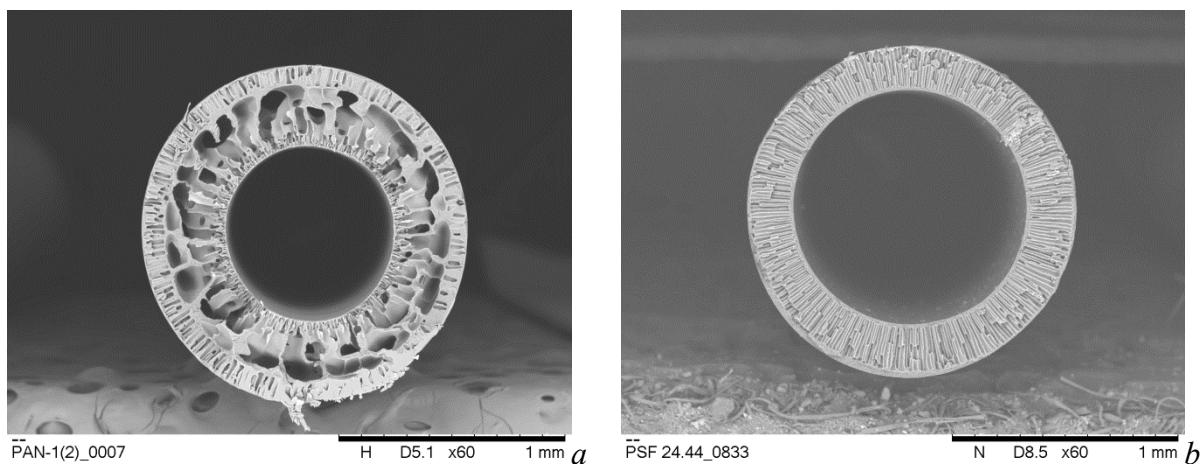


Fig. 4. Cross sectional SEM micrographs of hollow fiber membranes from a) PAN, b) PSF.

To estimate the parameters of the porous membrane structure the following values were determined: the size of the largest pore, the size of the smallest pore and the average pore size of the flow (Mean flow pore size - MFP), defined as the pore size for which 50% of the flow penetrated through the pores of a larger size and 50% of the flow penetrates through the smaller pores. Table 1 shows the above parameters for the investigated hollow fiber membranes. From Table 1 it is seen that the average size of pores, characterized by the parameter "Mean flow pore size" differs for the obtained membranes by no more than 8%.

The assessment of the effect of the chemical structure of the material on the high-voltage discharge currents in a highly inhomogeneous electric field through membranes with a given pore size was carried out in accordance with Fig. 1b at 15 kV high voltage and normal conditions. The measurement results are presented in Table 1. The data obtained show that for the case of the most common membrane materials PAN and PSF, no noticeable effect of the chemical structure of the material on the corona discharge current at identical pore parameters was found.

Table 1. Characteristics of hollow fiber membranes.

Membrane material	D_{out} , [mm]	D_{int} , [mm]	d , [mm]	Maximum pore size, [nm]	MFP, [nm]	Minimum pore size, [nm]	Average discharge current, [μ A]
PAN	1,43	0,73	0,35	182	14.9	13.9	15
PSF	1,45	1,01	0,22	22.4	13.9	12.9	16

Conclusion

The results obtained in the course of this work showed the fundamental possibility of using a inhomogeneous high-intensity electric field for non-destructive testing of the homogeneity of the porous structure of flat sheet and hollow fiber polymer membranes. An important advantage of this approach is the ability to identify areas of the membrane that contain defects and have increased conductivity. The nature of the arising defects can be studied in the future using modern destructive methods for analyzing the morphology of membranes, including transmission electron microscopy with layer-by-layer microtoming of samples. The revealed nature of defects will allow at the fundamental level to optimize the process of directed formation of the required porous structure of membranes and to intensify fundamental research in the development of new highly selective (defect-free) membranes of flat sheet and hollow fiber geometries. Using a pair of polysulfone and polyacrylonitrile hollow fiber membranes with the same average pore size, no noticeable effect of the membrane chemical structure on the corona discharge current was found.

Acknowledgements

The reported study was funded by RFBR, project number 20-08-00814.

References

- [1] Y. Zhang, Q. Fu, Algal fouling of microfiltration and ultrafiltration membranes and control strategies: A review, *Sep. Purif. Technol.* 203 (2018) 193–208.
- [2] D. Mancinelli, C. Hallé, Nano-filtration and ultra-filtration ceramic membranes for food processing: A mini review, *J. Membr. Sci. Technol.* 5(2) (2015) 2.
- [3] S.D. Bazhenov, A.V. Bilyukevich, A.V. Volkov, Gas-Liquid Hollow Fiber Membrane Contactors for Different Applications, *Fibers.* 6 (2018) 76.
- [4] A.W. Mohammad, Y.H. Teow, W.L. Ang, Y.T. Chung, D.L. Oatley-Radcliffe, N. Hilal, Nanofiltration membranes review: Recent advances and future prospects, *Desalination.* 356 (2015) 226–254.
- [5] S. Hu, R. Tong, Y. Bo, P. Ming, H. Yang, Fungal peritonitis in peritoneal dialysis: 5-year review from a North China center, *Infection.* 47(1) (2018) 35-43.
- [6] J.H. Jhaveri, Z.V.P. Murthy, A comprehensive review on anti-fouling nanocomposite membranes for pressure driven membrane separation processes, *Desalination.* 379 (2016) 137–154.
- [7] E.A. Grushevenko, I.L. Borisov, A.A. Knyazeva, V.V. Volkov, A.V. Volkov, Polyalkylmethylsiloxanes composite membranes for hydrocarbon/methane separation: Eight component mixed-gas permeation properties. *Sep. Purif. Technol.* 241 (2020) 116696.
- [8] C. Causserand, P. Aimar, 1.15–Characterization of Filtration Membranes, in: E. Drioli, L. Giorno. (Eds.), *Comprehensive Membrane Science and Engineering*, Elsevier Science, Amsterdam, 2010, pp. 311-334.
- [9] N. Peng, N. Widjojo, P. Sukitpaneelit, M.M. Teoh, G.G. Lipscomb, T.-S. Chung, J.-Y. Lai, Evolution of polymeric hollow fibers as sustainable technologies: Past, present, and future, *Prog. Polym. Sci.* 37(10) (2012) 1401–1424.
- [10] V.A. Kirsh, S.D. Bazhenov, Towards simulation of gas separation modules based on hollow fiber membranes, *J. Phys. Conf. Ser.* 1696 (2020) 012041.

-
- [11] V.A. Kirsch, S.D. Bazhenov, Numerical simulation of solute removal from a cross-flow past a row of parallel hollow-fiber membranes, *Sep. Purif. Technol.* 242 (2020) 116834.
- [12] S. Nakao, Determination of pore size and pore size distribution, *J. Membr. Sci.* 96(1-2) (1994) 131–165.
- [13] C. Zhao, X. Zhou, Y. Yue, Determination of pore size and pore size distribution on the surface of hollow-fiber filtration membranes: a review of methods, *Desalination.* 129(2) (2000) 107–123.
- [14] S. Bannwarth, H. Breisig, V. Houben, C. Oberschelp, M. Wessling, Membrane impedance porometry, *J. Membr. Sci.* 542 (2017) 352–366.
- [15] J.M. Sanz, D. Jardines, A. Bottino, G. Capannelli, A. Hernández, J.I. Calvo, Liquid–liquid porometry for an accurate membrane characterization, *Desalination.* 200(1-3) (2006) 195–197.
- [16] A. Jena, K. Gupta, Advances in Pore Structure Evaluation by Porometry, *Chem. Eng. Technol.* 33(8) (2010) 1241–1250.
- [17] K.R. Morison, A comparison of liquid–liquid porosimetry equations for evaluation of pore size distribution, *J. Membr. Sci.* 325(1) (2008) 301–310.
- [18] W. Piątkiewicz, S. Rosiński, D. Lewińska, J. Bukowski, W. Judycki, Determination of pore size distribution in hollow fibre membranes, *J. Membr. Sci.* 153 (1999) 91–102.
- [19] B. Lavi, A. Marmur, J. Bachmann, Porous Media Characterization by the Two-Liquid Method: Effect of Dynamic Contact Angle and Inertia, *Langmuir.* 24(5) (2008) 1918–1923.
- [20] V.P. Kasperchik, A.L. Yaskovich, A.V. Bil'dyukevich, *Ser. Krit. Tekhnol. Membr.* 28(4) (2005) 35.
- [21] D.N. Matveev, K.A. Kutuzov, V.P. Vasilevsky, Effect of Draw Ratio on the Morphology of Polysulfone Hollow Fiber Membranes, *Membranes and Membrane Technologies.* 2(6) (2020) 351–356.

Facile Fabrication of Porous and Hydrophilic Polystyrene Membranes Using Recycled Waste

Mostafa Khaled^{1,a*}, H. Noby^{1,b}, W.A. Aissa^{2,c}, A.H. El-Shazly^{3,4,d}

¹Materials Engineering and Mechanical Design, Faculty of Energy Engineering, Aswan University, Aswan, Egypt

²Mechanical Engineering, Faculty of Energy Engineering, Aswan University, Aswan, Egypt

³Chemical and Petrochemicals Engineering, Egypt-Japan University of Science and Technology (E-JUST), Alexandria, Egypt

⁴Chemical Engineering Department, Faculty of Engineering, Alexandria University, Alexandria, Egypt

^aMostafa_kh@aswu.edu.eg, ^bHussien379@energy.aswu.edu.eg,

^cWaessa@energy.aswu.edu.eg, ^dAhmed.elshazly@ejust.edu.eg

Keywords: porous membranes, polystyrene, hydrophilic, and recycled waste.

Abstract. Micro-porous semi-hydrophilic membranes were successfully fabricated using polystyrene waste by phase inversion casting. Four concentrations (20, 25, 30, and 35 wt%) of recycled high-impact polystyrene (HIPS-R) in N, N-dimethyl formamide (DMF) solution were employed to prepare the membranes. The effect of polystyrene concentration on the characteristics of the different membranes was thoroughly studied. Based on the Fourier transform infrared spectroscopy (FTIR) results, the chemical composition of HIPS-R was analogous to that of pure high-impact polystyrene HIPS raw material of the previous studies. Also, field-emission scanning electron microscopy (FESEM) was employed to study the morphology and porosity of the prepared membranes. The membranes cross-section showed a sponge structure with longitudinal macro voids. The solid walls around these voids have a sponge-like structure, especially for high concentration polystyrene membranes. Furthermore, the number of pores into the membrane surface decreased with the increase of polystyrene concentration. The membranes surface pores size was ranged from 150 nm to 550 nm with the different used concentrations. Water contact angle (CA) of the prepared membrane's surface was measured. All the measured CA of the prepared membranes, except the 35 wt% showed CA of 91°, showed a semi-hydrophilic behavior. Thus, the results suggest effective membranes could be obtained using recycled polystyrene. And then, solve the polymer waste accumulation problem in parallel with help in drinking water crisis solution.

1 Introduction

Polymers have distinctive characteristics such as lightweight, ease manufacturing, good mechanical properties, low cost, and even electrical conductivity as in conductive polymers [110]. Accordingly, their usage covers several fields and applications. Plastics are produced at a rate of 230 million tons in the year and is expected to reach 400 million tons in 2020 due to fast growth in the population every year[1]. Besides, plastics represent about 12 % of the solid waste. Thus, plastic recycling is highly considered to limit the side effects of polymer waste. Efficient treatment of waste polymers is still a serious challenge. There are enormous methods to eliminate plastics waste amounts such as combustion or burying underground. Unfortunately, these methods have negative effects on the environment. Consequently, scientists concentrate on innovating new methods for polymers recycling [1]. Among these polymers that can be recycled, high-impact polystyrene (HIPS) which is formed by the polybutadiene rubber and polystyrene (PS) interaction.

HIPS showed significant advantages such as high impact resistance, stability, and simple preparation [2].

Dimethylformamide was used as a solvent in this study. Dimethylformamide is an organic solvent produced in large quantities throughout the world. Dimethylformamide is widely used in the chemical

industry as a solvent, an intermediate, and an additive, with the largest quantities used in the production of acrylic fibers and polyurethanes. Dimethylformamide is also used in the production of pharmaceutical products. Because of its complete solubility in water, dimethylformamide is noted to move readily through soils. Concerning effects on organisms in the environment, the limited data available suggest low toxicity for organisms [15].

Polymers were used widely in separation applications [4-7, 11-14]. The preparation of PS membranes was investigated in enormous studies using different methods due to its effective performance for many applications. Zhuang et al. fabricated flat sheet membranes from diverse types of waste PS for the gas separation [3]. It was found that the recycled high-impact polystyrene (HIPS-R) displayed good thermal stability and higher gas permeation performance [4]. Garcia et al. studied the application of HIPS-R flat sheet membranes in low-pressure membrane processes [2]. An asymmetric structure with slightly higher porosity, when compared to the commercial HIPS membranes, were successfully obtained [2]. Bussi et al. fabricated PS membranes by phase inversion method with finger-like structure cross-sectional [5]. Ke et al. used electrospinning method to fabricate nanofibrous PS membranes with a superhydrophobic surface [6]. Microporous PS membranes with enhanced surface hydrophobicity were successfully synthesized in [7].

In the current work, HIPS-R was used to fabricate membranes by phase inversion method. This study aims to assess the feasibility of fabricating membranes from recycled plastic materials with significant enough characteristics to be used in water treatment applications. The effect of the PS concentration on the physical and chemical properties of the produced membranes was studied. The prepared membranes were characterized using FTIR, SEM, and surface contact angle (CA) measurements.

2 Materials and Methods

2.1. Materials

HIPS-R cups obtained from the local Egyptian market were used as the membrane's polymer base material. The cups were washed and dried before use, cut into small square pieces (5 mm average side length), ultrasonicated in distilled water, and dried overnight at 75 °C. N, N-dimethyl formamide (DMF), (Sigma Aldrich) was employed as the organic solvent. Distilled water was utilized for washing and solution preparation processes.

2.2. HIPS-R membranes preparation

Membranes were prepared using non-solvent induced phase separation (NIPS) method as shown in Fig. 1. The homogeneous polymer dope solution was prepared using HIPS-R in DMF. The polymer solutions concentrations were adjusted (20, 25, 30, and 35 wt%) in 10 mL DMF solvent. The mixtures were stirred at 50 °C for 3 h until a homogeneous solution was obtained. The solutions were then cast on glass slides with a 200 µm doctor blade at room temperature. They were immersed in a coagulation bath (distilled water at 20 °C) for 30 min to complete the precipitation. Then the membranes were washed with denoised water and dried overnight at 70 °C.

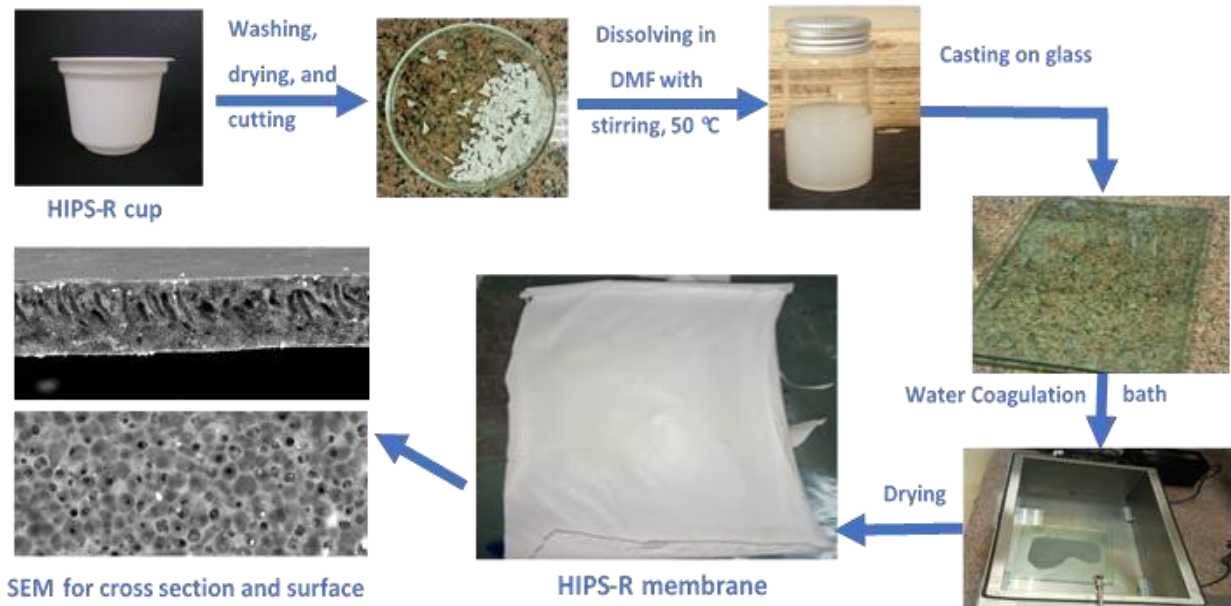


Fig. 1. Schematic diagram for a start to end HIPS-R membrane preparation process.

2.3. Membrane characterization

Field-emission scanning electron microscopy (FESEM, FEI Quanta 200 scanning electron microscope, FEI Company BV, Netherlands) was used to observe the surface and cross-sectional morphology of the prepared membranes. Also, image analysis software (Image-J, National institutes of health, USA) was applied to analyze the membranes mean pore size and pores size distribution. CA measurements (OCA 15EC Contact angle model, Data Physics Instrument GmbH) were employed to show the hydrophilicity of the surfaces of the prepared membranes with water droplets. FTIR analysis (VERTEX 70, Bruker, Germany) was used to check the purity of the prepared membranes by comparing with the commercial HIPS. Spectra were recorded in the range from 400 to 4000 cm^{-1} .

The average porosity of the surfaces of the membrane was calculated by wet-dry weighting method. A small part of each membrane was soaked in water for 48 h until water filled the pores. Then, the excess water on the sample surface was removed. The surface porosity for each membrane was calculated using Eq. 1:

$$\% \text{ porosity} = \frac{W_w - W_D}{\frac{\rho_w}{W_w - W_D} + \frac{W_D}{\rho_p}} * 100 \quad (1)$$

where, W_w and W_D are the weight of the wet and dry samples (g), respectively. ρ_w is the water density at room temperature (g/cm^3), and ρ_p is the density of the polymer (g/cm^3).

3. Results and Discussion

3.1 FESEM

SEM images for the membranes cross-sectional section are shown in Fig. 2. The membranes cross sections showed a sponge-like structure with noticeable longitudinal macrovoids. These macrovoids are formed due to the high exchange rate between DMF (solvent) and distilled water (non-solvent) due to the high miscibility, i.e., diffusivity, between them. The solid walls around these voids have a sponge-like structure, especially for high concentration polystyrene membranes.

The kinetic changes in the phase inversion process are very crucial for the formation of the membrane structure. The slow exchange rate between the solvent/ nonsolvent interfaces, i.e., the immersion/precipitation process, is usually the reason for the formation of sponge shape [2]. Also, slow rate suppresses the formation of macrovoids in the cross-section. Furthermore, the instantaneous precipitation supports the formation of a thin layer on the surface of the membrane. Accordingly, the macrovoids formation is extended till the upper surface of the cross-section. This layer could be thick

if the separation is done in a high exchange rate [2]. The surface pores will be blocked if a thick surface layer is formed. Which in turn, will significantly decrease the effectiveness of the membrane.

The solubility difference between the solvent/ nonsolvent interface dramatically influences the membrane separation process. It was clearly stated that water and DMF showed a high mutual attraction due to the high solubility difference between them. Accordingly, the diffusivity between water and DMF will be significantly high [2]. Which in turn will cause instantaneous separation and macrovoids will appear. Increasing the PS percentage in the mixture may lower the solution viscosity solvent/ nonsolvent diffusivity. Accordingly, the macrovoids decreased with the rise in the PS concentration as shown in Fig. 2.

SEM images of membranes surface are shown in Fig. 3. It was clearly illustrated that the surface membrane porosity reduced with the rise of polystyrene concentration. The membranes surface pores size was ranged from 150 nm to 550 nm with the different concentrations used. Also, the pores appeared clearly in the low PS concentration membrane. The pores are blocked with the rise in the PS concentration. In the high PS concentration membranes (30 and 35 wt%), spots of holes could be seen. These spots may be related to the high concentration of impurities with high HIPS concentration.

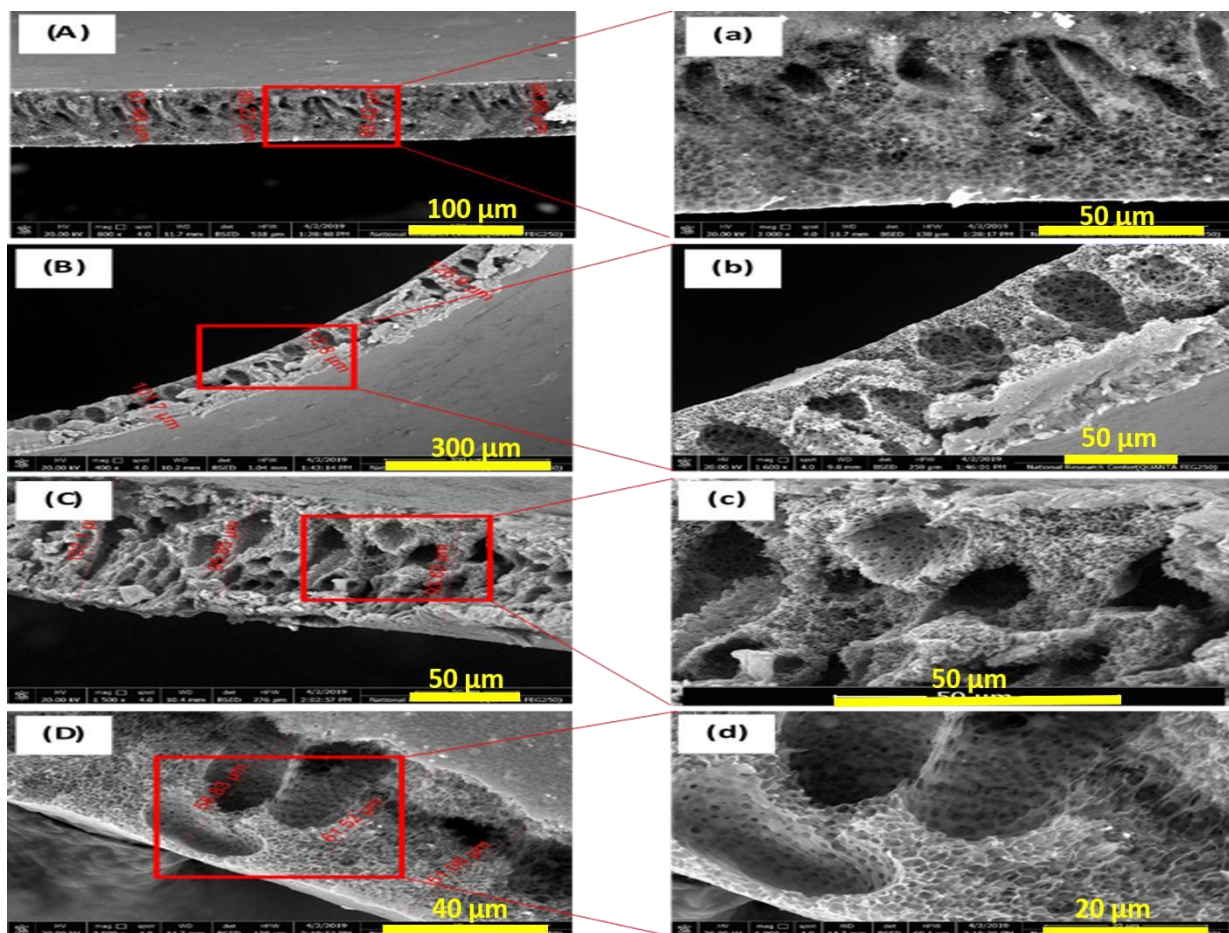


Fig. 2. SEM images of cross-sections of HIPS-R membranes; (A,a) 20 wt%, (B,b) 25 wt%, (C,c) 30 wt%, and (D,d) 35wt%.

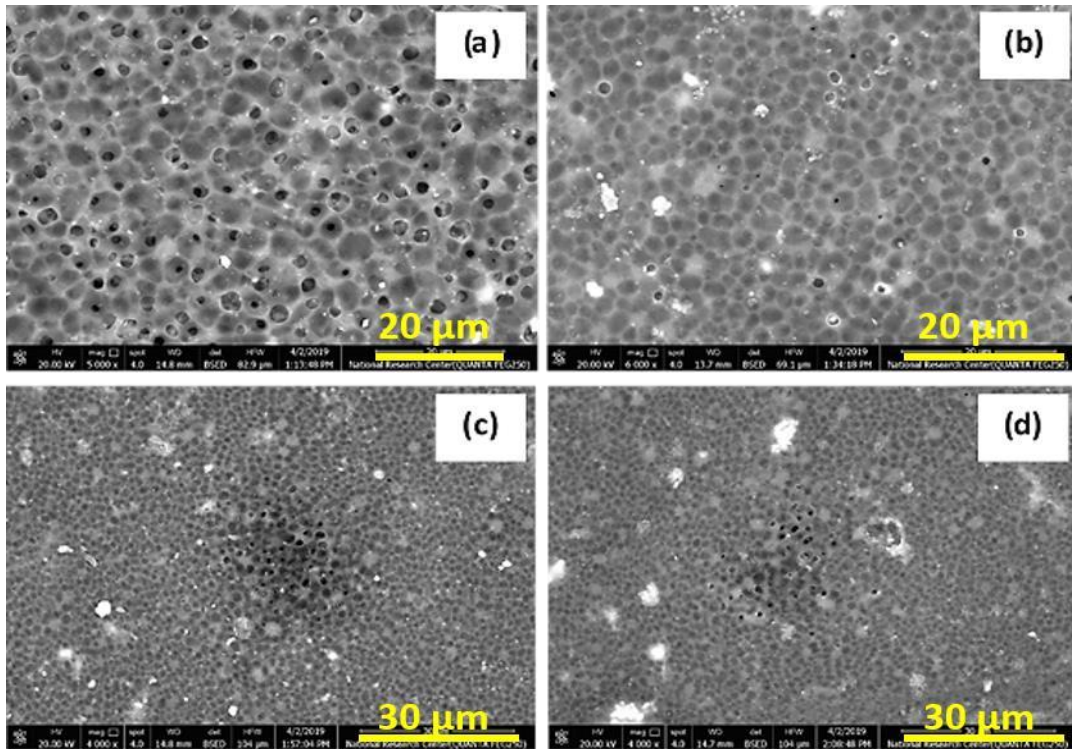


Fig. 3. SEM of HIPS-R membranes surfaces; (a) 20 wt%, (b) 25 wt%, (c), 30 wt%, and (d) 35wt %.

3.2 Membrane pore size and pore size distribution

Figure. 4 showed the pores diameter distribution of the produced membranes. The low PS concentration membranes showed that the pore diameter less than 1.5 μm represented the majority of the pores (see Fig. 4a). The pore diameter distribution illustrated that the main pore size decreased with the rise of HIPS-R concentration.

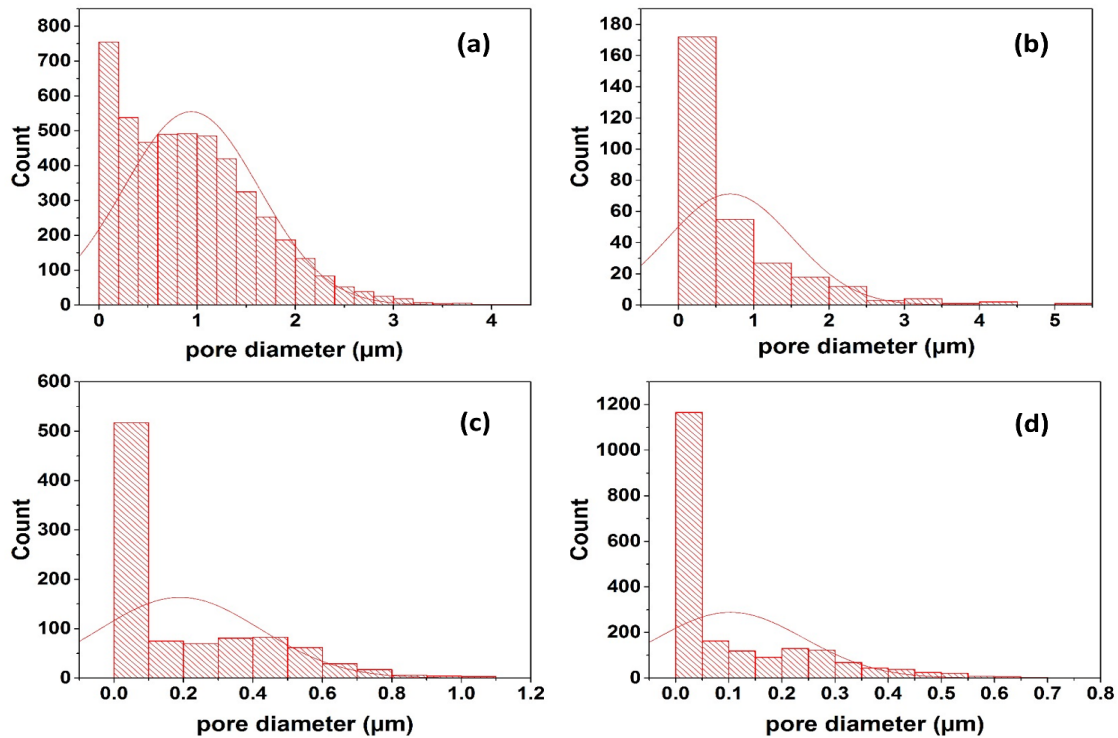


Fig. 4. Pore diameter distribution of the produced membrane surface using HIPS-R concentration of (a) 20 wt %, (b) 25 wt %, (c) 30 wt %, and (d) 35 wt %.

3.3 Membrane porosity

Surface porosity values of the different prepared membranes are shown in Fig. 5. It was clearly shown that the membrane with the PS concentration of 20 wt % displayed the largest surface porosity (72.25 %). The porosity declined with the HIPS-R concentrations rise. The large size of the pores and the formation of a large number of macrovoids in case of low PS concentration membranes may be the direct reason for the accomplished high porosity. With the increase of PS concentration, the pores size and numbers of macrovoids reduced which in turn lessened the overall porosity of the membrane.

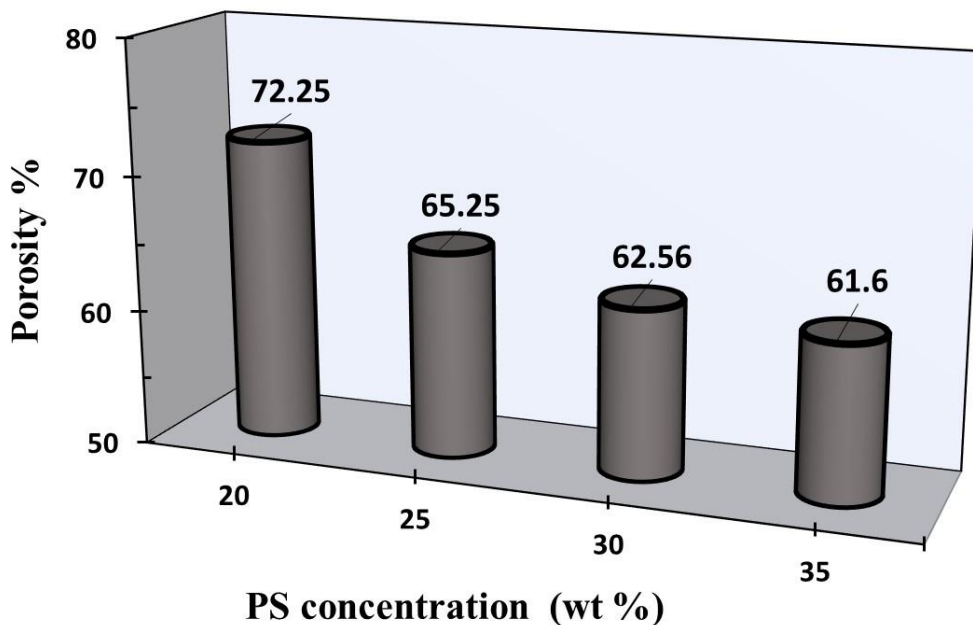


Fig. 5. Porosity of the produced membranes using HIPS-R at different concentrations.

3.4 Contact angle measurements

Water contact angle (CA) of the prepared membrane's surface was measured. All the measured CA of the prepared membranes, except the 35 wt% showed CA of 91° , showed a hydrophilic or semi-hydrophilic behavior as shown in Fig. 6. The CA increased with the rise of the HIPS-R concentration. The increase of HIPS-R concentration will raise the contaminant percentage in the membrane surface. The direct contact between water and the surface contaminant may play the key rule in the CA increase. Also, the change of the membrane surface due to the change in the size of the pores may represent another candidate reason for the CA rise.

3.5 Chemical structure

The absorbance FTIR spectra of the different membranes were recorded in Fig. 7. It can be observed that the chemical composition of HIPS-R (Fig. 7b) was analogous to that of pure HIPS. The peaks at 2917.18 , 3082 , and 3026 cm^{-1} correspond to the C-H bond stretching vibrations. The absorption peaks at 1595.81 and 1446.59 cm^{-1} were related to the aromatic C=C vibrations. The presence of a peak at 1718 cm^{-1} , attributed to the stretching vibration of C=O groups, can demonstrate the presence of polybutadiene [8], [9]. The presence of additives containing silicon was also observed by the long-chain Si-CH₂-R groups located at 1248 cm^{-1} , peak at 1096 cm^{-1} assigned to Si-O-C bond, and the band related to the stretching vibrations of the Si-O bond at 880 cm^{-1} [10].

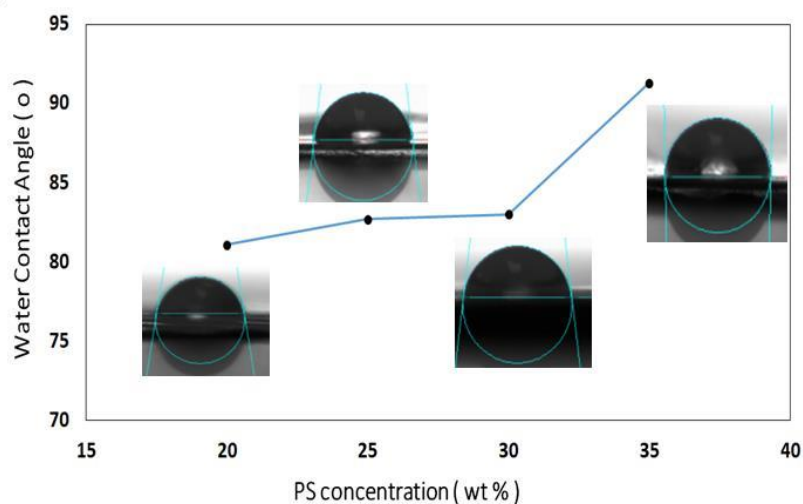


Fig. 6. Water droplets contact angles of the prepared membranes using different HIPS-R concentration.

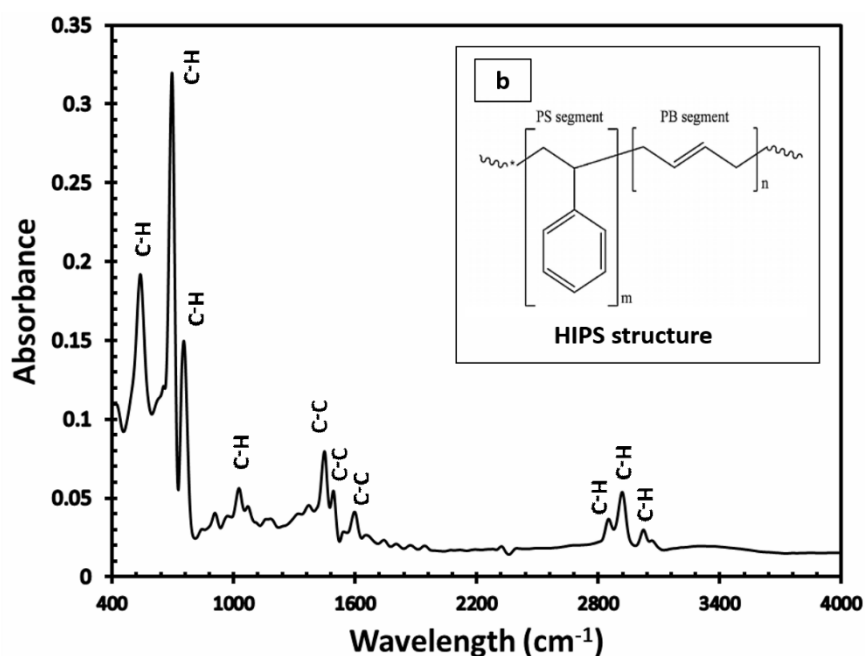


Fig. 7. FTIR spectra of the HIPS-R and (intersect b) represents the chemical structure of HIPS.

Conclusion

Hydrophilic flat sheet membranes were successfully fabricated from recycled high impact polystyrene. Different membranes were prepared using different polystyrene concentration in DMF solution. These membranes showed different cross-section structure and surface pores size distribution. The surface porosity decreased with the rise of HIPS-R concentrations. The crosssection of the membranes had a large macrovoids surrounded by sponge-like structure solid walls. The diffusivity of the DMF/HIPS-R solution with the coagulant, water, effect on the formation of the macrovoids and the sponge structure was approved. According to the low diffusivity of the solvent/nonsolvent system with the high HIPS-R concentration, the porosity gradually diminished from 72.25 to 61.6 % when the concentration raised from 20 to 35 wt %, respectively. Contact angle measurements showed that the membranes had a semi-hydrophilic surface. Finally, these results suggested that polystyrene wastes can be used to prepare effective flat sheet membranes.

Consequently, a one-step solution was presented in this study to solve both challenges of polymer waste accumulation and water treatment.

References

- [1] Y. Zare, "Recent progress on preparation and properties of nanocomposites from recycled polymers: A review," *Waste Manag.*, vol. 33, no. 3, pp. 598–604, 2013 .
- [2] J. Garcia-ivars, X. Wang-xu, and M. Iborra-clar, "Application of post-consumer recycled high-impact polystyrene in the preparation of phase-inversion membranes for low-pressure membrane processes," *Sep. Purif. Technol.*, vol. 175, pp. 340–351, 2017 .
- [3] G. L. Zhuang, H. H. Tseng, and M. Y. Wey, "Feasibility of using waste polystyrene as a membrane material for gas separation," *Chem. Eng. Res. Des.*, vol. 111, no. C, pp. 204–217, 2016 .
- [4] Y. Bussi, S. Golan, C. G. Dosoretz, and M. S. Eisen, "Synthesis, characterization and performance of polystyrene/PMMA blend membranes for potential water treatment," *Desalination*, vol. 431, no. December 2017, pp. 35–46, 2018 .
- [5] H. Ke et al., "Electrospun polystyrene nanofibrous membranes for direct contact membrane distillation," *J. Memb. Sci.*, vol. 515, pp. 86–97, 2016 .
- [6] Y. Wang et al., "Enhanced performance of superhydrophobic polypropylene membrane with modified antifouling surface for high salinity water treatment," *Sep. Purif. Technol.*, 2018 .
- [7] A. M. Bernardes, J. Z. Ferreira, and C. A. Ferreira, "High-impact polystyrene / polyaniline membranes for acid solution treatment by electrodialysis: Preparation, evaluation, and chemical calculation," vol. 320, pp. 52–61, 2008 .
- [8] K. Hu et al., "Synthesis, Structure, and Properties of High-Impact Polystyrene / Octavinyl Polyhedral Oligomeric Silsesquioxane Nanocomposites," pp. 1–7, 2014 .
- [9] J. P. Matinlinna, S. Areva, L. V. J. Lassila, and P. K. Vallittu, "Characterization of siloxane films on titanium substrate derived from three aminosilanes," pp. 1314–1322, 2004 .
- [10] H. Noby, A.H. El-Shazly, M.F. Elkady, M. Ohshima, Novel preparation of self-assembled HCl-doped polyaniline nanotubes using compressed CO₂-assisted polymerization, *Poly.*, 156 , 71-75, 2018.
- [11] H. Noby, A. H. El-Shazly, M. F. Elkady, and M. Ohshima, "Adsorption Profiles of Acid Dye Using Synthesized Polyaniline Nanostructure with Different Morphologies", *J. Chem. Eng. Jpn.*, 50, 170177, 2017.
- [12] I. V. Korolkov, Y. G. Gorin, A. B. Yeszhanov , A. L. Kozlovskiy, M. V. Zdorovets, "Preparation of PET track-etched membranes for membrane distillation by photo-induced graft polymerization", *Mate. Chem. Phys.*, 205, 55-63, 2018.
- [13] M. Fujiwara, "Water desalination using visible light by disperse red 1 modified PTFE membrane", *Desal.*, 404, 79–86, 2017.
- [14] K. Buruga, J. T. Kalathi, K. H. Kim, Y. S. Ok, B. Danil, "Polystyrene-halloysite nano tube membranes for water purification", *J. Ind. Eng. Chem.*, 61, 169–180, 2018.
- [15] A. Bainova, "Dimethylformamide", *World Health Organization & International Programme on Chemical Safety.*, 1991.

Effect of Sericin Additive on Cellulose Acetate Membrane Morphology and Protein Rejection

HIZBA Waheed^{1,a*}, AMIR Mukhtar^{2,b}

¹Department of Chemical Engineering, Wah engineering College, University of wah, Wah Cantt, 47040, Pakistan

²School of Chemical and Materials Engineering (SCME),
National University of Sciences and Technology, H-12, 44000, Islamabad, Pakistan

^{a*}hizba.waheed@uow.edu.pk, ^bdrameermukhtar@gmail.com

Keywords: Cellulose Acetate blended Membrane, Sericin, BSA rejection.

Abstract. Cellulose acetate (CA) membranes are synthesized for filtration purpose. The hydrophilic sericin macromolecule is blended with CA to analyze the enhancement of protein rejection. Increase in hydrophilicity, water permeation and protein rejection was studied by using contact angle, pure water flux (PWF) and Bovine serum albumin (BSA) permeation respectively. Surface modification was examined using SEM and AFM. The results show the homogenous blending of sericin in CA matrix and effective fabrication of membranes. In order to gauge the efficiency of casted membranes in protein filtration and separation, water flux and protein rejection were studied. The concentration of sericine protein was altered in CA polymeric solution that imparts variable properties to fabricated membrane samples. Increment in wt. % of sericine up to 7.5 in polymer dope solution, enhances BSA rejection to the limit of 96%. The amino linkages between sericine and the BSA of feed resulted in the holding of protein by sericine, which leads to low permeation of BSA via CA-Sericine membrane M4.

Introduction

Utilization of membrane processes for biological separation is a primordial process. With the advent to new methods in membrane technology, membranes occupy a vital place in modern industries [1]. The research concerning preparation, characterization and applicability of polymeric membranes is evolving tremendously. Membrane technology is being utilized in key areas of interest like water purification, artificial organs, fuel cells, membrane reactors, composite materials [2].

Various polymers are used for the preparation of membranes including polyacrylonitrile (PAN), polymethyl methacrylate (PMMA), polyamide (PA), polyvinylalcohol (PVA) [3-7], cellulose and cellulose derivatives. Cellulose is a colorless and odorless polymer but possesses excellent characteristics like, fine mechanical strength, superior biocompatibility and hydrophilicity, high absorption potential and relatively better thermal resistance [8]. Acetylation of Cellulose yield variable derivative with variable degrees of substitution (DS). Typically, the DS is 2.48 because of its molecular weight, solvation behavior in a range of polar organic solvents and flow characteristics [9]. It is utilized in membranes preparation for almost all separation processes like ultrafiltration (UF), microfiltration (MF), reverse osmosis (RO) and nano filtration (NF).

Polymer solution versatility and convenient membrane fabrication processes make membrane technology more applicable and practical technique for separation procedures. The characteristics of cellulosic membranes are manageable via synthesis of filtering aids (membrane) with measured porosity. The use of organic and inorganic additives in casting solutions is a latest and accepted approach for controlling membrane's structure and pore size. Membranes are commonly applied for the clearance, purification and fractionation of protein-containing solutions including proteins produced via fermentation, proteinaceous products from other industrial processes and for the recovery of extracellular protein. Competency of membrane for protein separation is the defining parameter for protein filtration. For any case, improved flow rates of permeates, sieving capacity, size exclusion and selectivity of membrane will complement to the financial side of process [10-11].